



Review

Regeneration mechanism, modification strategy, and environment application of layered double hydroxides: Insights based on memory effect



Haoyang Ye^a, Shiyu Liu^a, Deyou Yu^b, Xuerong Zhou^a, Lei Qin^{a,*}, Cui Lai^{a,*}, Fanzhi Qin^a, Mingming Zhang^a, Wenjing Chen^a, Wenfang Chen^a, Ling Xiang^a

^a College of Environmental Science and Engineering, Hunan University and Key Laboratory of Environmental Biology and Pollution Control, Hunan University, Ministry of Education, Changsha, Hunan 410082, PR China

^b Key Laboratory of Advanced Textile Materials and Manufacturing Technology, Ministry of Education, School of Textile Science and Engineering, Zhejiang Sci-Tech University, Hangzhou 310018, PR China

ARTICLE INFO

Article history:

Received 29 July 2021

Accepted 29 September 2021

Available online 12 October 2021

Keywords:

Layered double hydroxide

Layered double oxide

Catalysis

Adsorption

Memory effect

ABSTRACT

Layered double hydroxides (LDHs), are ideal inorganic materials for versatile fields, such as catalysis, energy, and medicine. Memory effect means the ability of reconstruction into their initial structure after decomposition treatment for some special materials. Based on the unique property, the layered structure can be regenerated from the calcined LDHs (layered double oxide, LDO) in an aqueous solution or moist air. This effect provides a new paradigm for modification of LDHs, increasing the abundance of active sites in LDHs as well as preserves original active sites for multifunctional environmental applications. Therefore, this review summarizes the memory effect of LDHs from basic mechanisms to real applications. Firstly, various kinds of active sites on LDHs/LDOs and the importance of sites structure are concluded. Secondly, the modification methods of LDHs are briefly introduced and the characteristics of memory effect are summarized. Then, the mechanism of chemical reaction, topology, and thermodynamics of memory effect are discussed as well as the microscopic mechanism of memory effect through theoretical chemical calculation. The influencing factors and applications in environmental remediation are also presented. Finally, the challenges and prospects of memory effect-based LDHs are proposed. We hope the review could open a new path for the environmental application of memory effect-based LDHs.

© 2021 Elsevier B.V. All rights reserved.

Contents

1. Introduction	2
2. The activity of LDHs/LDOs and its memory effect origin	3
2.1. Strategies in the modification of LDH-based materials	3
2.1.1. Assembly (self-assembly)	3
2.1.2. Ion exchange	4
2.1.3. Delamination	4
2.2. Activity and reactivity of LDHs/LDOs	4
2.2.1. Layer metal ions	4
2.2.2. Interlayer molecules and anions	4
2.2.3. Active structure	5
2.3. A special performance: memory effect	7
2.3.1. Monitoring of memory effect	7
2.3.2. Chemical reaction and topological processes: the origin of memory effect	9
2.3.3. Thermodynamics and theoretical calculation chemistry: a new horizon for memory effect	10
3. Influence factors of memory effect	12

* Corresponding authors.

E-mail addresses: leiqin@hnu.edu.cn (L. Qin), laicui@hnu.edu.cn (C. Lai).

<https://doi.org/10.1016/j.ccr.2021.214253>

0010-8545/© 2021 Elsevier B.V. All rights reserved.

3.1. Temperature	12
3.2. pH	13
3.3. Metal composition	13
3.4. Reconstruction anion and molecules	13
4. Environmental applications of LDH-based materials with memory effect	15
4.1. Adsorption application	15
4.2. Catalytic applications	18
4.3. The suppression of the memory effect	19
5. Challenges and prospects	19
Declaration of Competing Interest	20
Acknowledgments	20
References	20

1. Introduction

The rapid development of industrialization and urbanization has caused a series of problems, and environmental pollution is one of the most serious risks. Heavy metals, persistent organic pollutants (POPs), volatile organic compounds (VOCs), and emerging pollutants have deeply affected the ecosystem and human wellness. Among them, emerging pollutants have attracted increasing attention, because most of them are far more resistive than the traditional pollutants with long-term risk. Emerging pollutants are a tremendous family (*i.e.*, analgesics, antibiotics, polybrominated diphenyl ether), having significantly toxic and hormone-disrupting properties. They are related to diseases in the population, occurrence of superbugs and environmental allergens [1]. Therefore, it is urgent to prevent and remove the emerging pollutants. A variety of methods are available for the removal of emerging pollutants, such as adsorption [2], Fenton oxidation [3],

electrocatalysis [4], and photocatalysis [5], where the functional materials are the key for carrying out these approaches [6–8].

Layered double hydroxides (LDHs) are a kind of bimetallic hydroxide materials with layered structure and exchangeable interlayer anion, which are widely applied in medicine [9–11], civil engineering [12,13], energy engineering [14,15], and environmental remediation [16]. Moreover, the unique properties of LDHs, such as uniform metal dispersion, economic cost, adjustable metal ion composition, and variable layer spacing, have attracted wide interests of many researchers [17–19]. Particularly, LDHs have shown high efficiency performance in adsorption and catalysis because of their tunable composition and flexible structure in the environmental remediation, which can provide many active sites [18,20–24]. However, the original LDHs are still unable to meet the requirements of multi-function, stability, controllability, and reusability. Thus, modification is often necessary for improving the performance of LDHs. Many common modification methods

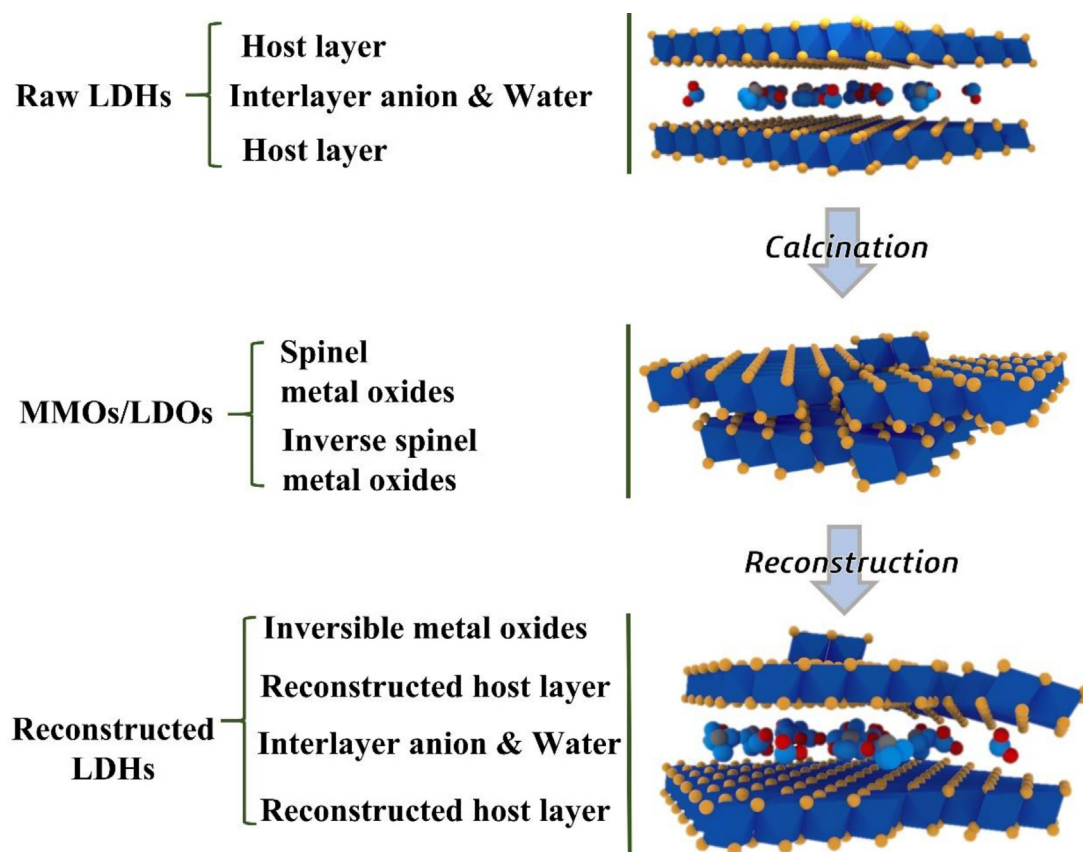


Fig. 1. The basic process of memory effect.

are developed, including ion exchange [25], assembly [26], delamination [27], and thermal treatment [28]. Thermal treatment such as calcination is a notable one among above methods. After calcination processing, the layered structure of LDHs will be transferred into mixed metal oxides (MMOs) or layered double oxides (LDOs), which no longer show a classic layered structure like LDHs, but still exhibit well in catalysis, adsorption, and control of water eutrophication [26,29,30].

Some LDOs can be converted back to layered structure like the original LDHs (ex-LDHs) in aqueous solution or steam environments [29–31]. This structure transformation phenomenon is named as memory effect. In a typical memory effect process, LDOs are contacted with solution or humidity, then they will reconstruct layered structure and recapture the interlayer anions. Therefore, the memory effect can enhance the decontamination or performance through promoting the captured ability to target matter [32], indicating that it has the potential to be applied to environmental remediation via catalysis processes [33,34]. Besides, some irrecoverable metal oxides are still retained in the reconstructed structure (Fig. 1). However, few researches related to memory effect modified LDHs linked the mechanism to real application, or only simply regards them as a side-effect of LDOs applications. For example, the mechanism of the memory effect on LDHs has been simply postulated in some studies [35,36]. It has also been tentatively proposed that the memory effect is a “direct synthesis” [37]. In addition, the research on the influencing factors of memory effect has been carried out for a long time, but there is still a lack of systematic summary. Its application conditions and relevant mechanism are not summarized in detail. Besides, achievements in computational chemistry help to explain the mechanism of the memory effect, while those achievements are usually ignored in previous reviews.

Hence, in this review, we first summarize the active sites of LDHs and LDOs related to the memory effect. Then, the conventional modification strategies of LDHs/LDOs are compared, and the structure characterizations corresponding to memory effect are also discussed. More importantly, the mechanism of memory effect for LDH-based materials is discussed in detail. Subsequently, conditions affecting the reconstruction of LDHs such as calcine temperature, interlayer anion, pH, surface charge, hydration, and layer metal composition are explored. Moreover, the applications

of memory effect-based LDHs in adsorption and catalysis are also reviewed, and the suppression strategies of memory effect are also suggested in brief. Finally, the perspectives and barriers for memory effect-based LDHs in environment remediation are proposed.

2. The activity of LDHs/LDOs and its memory effect origin

2.1. Strategies in the modification of LDH-based materials

The most crucial aims for the modification of LDH-based materials are to add active sites and improve their stability, reusability, and functionality. Most modification methods can not only preserve the memory effect, but also sometimes enhance the utilization of the active sites caused by the memory effect. Calcining LDHs into LDOs is the main strategy related to memory effect, which will be discussed in section 2.3. Other modification ways which are closely related to the application or mechanism of memory effect, such as assembly, ion exchange, and delamination are described in this section.

2.1.1. Assembly (self-assembly)

Assembly is an attractive strategy to develop bifunctional materials. During the assembly process, LDHs are integrated with other host materials to synthesize new materials. These host materials can be used as semiconductor materials, carbon materials, metal materials, or even layers from other LDHs [38–40]. When exogenous materials are used as the substrates, they are soaked in the precursor salt solution to make LDHs grow on the substrate by coprecipitation [41,42]. For example, Liu et al. grew ZnAl-LDH on carbon aerogel and utilized the compound for tellurite removal (Fig. 2a). LDHs can also be used as substrates [43], Chen et al. synthesized electrospun nanofiber membrane on LDH for copper adsorption (Fig. 2b) [43]. The modification method of assembly is widely used, and in most cases, the loading process does not affect the memory effect [44]. In other words, the memory effect of using the template method to synthesize the LDH with a specific shape ensures that the material can still be used to maintain the structure of the LDH after using the heat to remove the template or carrier [45]. This means another property brought about by memory effect: self-assembly. Efficient drug carriers or catalysts can be syn-

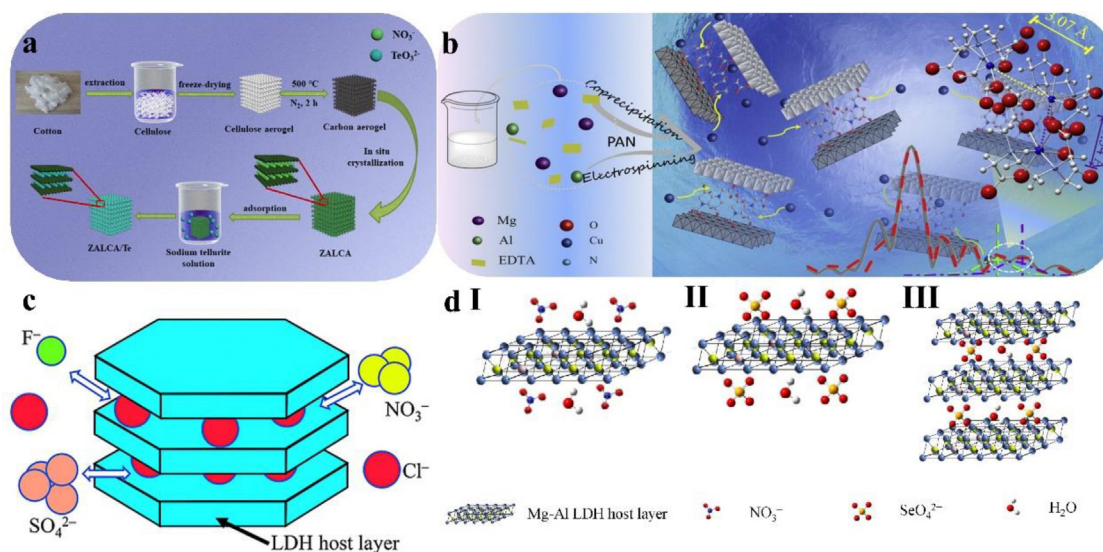


Fig. 2. LDH modification strategies a) grew LDH on carbon aerogel [42], b) grew PAN on MgAl-EDTA-LDH [43], c) anion exchange of LDH [52], d) adsorption of SeO_4^{2-} by MgAl-LDH nanosheet: I) original LDH layer, II) used LDH layer, III) LDH structure after adsorption [55].

thesized rapidly by self-assembly [45,46]. A self-assembly process with memory effect can also fix metal oxides to LDH [47].

2.1.2. Ion exchange

LDHs and LDOs have a strong ability of ion exchange. Interlayer anions can be replaced by another anion to form a new active site on the premise of satisfying a certain exchange sequence (Fig. 2c). Easy operation and a wide range of applications are the most obvious advantages of ion exchange. Ali et al. inserted MoS_4^{2-} into Fe-LDH to enhance its rate of electron transfer during activation of persulfate and accelerate the redox cycle of Fe [48]. From another point, ion exchange and memory effect can occur simultaneously, this also implies that the problem of ion exchange should be noticed during the modification process of LDHs by memory effect. However, compared with the complete loss of anions from the layer structure by memory effect and anion re-intercalation by reconstruction, such ion exchange is limited by the exchange sequence. In addition, the interference of carbonates or phosphates is always unavoidable in ion exchange [25,28,49–52]. The main connection between memory effect and ion exchange is the manipulation of interlayer anions. Both of them can modify interlayer anions. However, ion exchange is strictly limited by the exchange order and is more complicated in operation. The original interlayer anions (usually carbonate) can be completely erased by calcination, and then the interlayer anion exchange can be achieved by immersing in the target anion solution during the memory effect process.

2.1.3. Delamination

Monolayer LDHs can be utilized as ultra-thin nanosheet material or be formed colloidal solution as a precursor of coating materials [53–56]. Usually, delamination happens in the ultrasonic oscillation and thermal treatment in a specific solvent [27,53,57], LDHs will be eventually peeled into monolayer material, which shows the characteristics of colloid solution [53]. Kameda et al. delaminated MgAl-LDH in deionized water to form an LDH nanosheet successfully [55]. Delamination-reconstruction could complete the loading of the active sites. Nityashree. N and Premitha Menezes synthesized Pt-doped MgAl-LDH. MgAl-LDH was delaminated in 1-butanol sonicating and Pt nanoparticles were dispersed in the same condition. Finally, mixing and rotatory evaporation were performed until dry. The layers were recombined into an LDH containing Pt [27]. The mechanism of delamination-reconstruction process is similar to the memory effect. All of them involve nucleation and aggregation in the topological transformation of the layers during memory effect reconstruction.

2.2. Activity and reactivity of LDHs/LDOs

The origin activity of LDHs/LDOs is determined by active sites. In general, metal ions, surface defects, interlayer substances (molecules and anions), surface hydroxyl groups, and sheet charge can act as the main active sites in LDHs/LDOs. Other structures such as pore structure also influence its activity. Tracking the activity origins of LDHs/LDOs may be a key to clarify the mechanism of performance improvement by memory effect. Moreover, when understanding the origin of active sites in LDHs/LDO, potential usages of these materials will be revealed.

2.2.1. Layer metal ions

The active sites are provided by the metal ions constituting LDHs. Base metals in LDHs layer showed more unique performance compared to noble metals as the catalyst or chemical sensing [58]. The LDHs/LDOs structure immobilizes these metal ions and provides conditions for heterogeneous reactions. Therefore, LDHs materials are utilized as dispersed atom catalyst with

lower cost and metal load capacity than noble metal and higher activity [59–63]. Meanwhile, the structure of LDHs/LDOs provides a possibility to enhance the catalytic performance of metal ions because of the co-exist anions, hydroxyl or other co-catalysis structures. For example, metal ions in LDHs could act as catalyst in radical generation from surface hydroxyl [64–66]. A CuNiSn-LDH was developed by Wang et al. to facilitate Fenton reaction for phenol removal. Cu ions served as the primary active sites for hydroxyl radical ($\text{HO}\cdot$) generation [66,67]. Similarly, the work of Guo et al. uncovered the Co(II) and Cu(II) in CoCu-LDH membrane were the redox center of persulfate activation in sulfate radical-advanced oxidation process (SR-AOP) [65]. Meanwhile, the original LDHs do not affect the catalytic mechanism of metal ions [68,69].

Metal active sites and bimetallic synergistic effect are also able to explain the activity of LDHs/LDOs [70]. Sn in the mentioned CuNi-LDH catalyst could accelerate the redox cycle of Cu by accelerating electron transfer [63]. A MnFeCo-LDO performed high efficiency in low-temperature NO_x reduction due to the high content of surface Mn^{4+} species and the co-existence of Co and Fe [71]. Moreover, Fe offered surface Lewis acid sites for the selective reduction in the previous reports [72]. Yao et al. reported a CoMn-LDO for Fenton-like process, in which the presence of Mn(II) and Mn(III) allowed the rapid reduction of Co(III) to Co(II), improving the utilization of active sites [68]. Similarly, metal ions in LDOs can enhance photocatalytic activity. For example, Liu et al. utilized ZnLn-LDH derived ZnLn-LDO in photocatalysis. The bimetallic combination of Zn oxide and Ln oxide enhanced the optical response range of the material, with the basic mechanism of h^+ photogenerated by the electronic transition. The Zn/Ln oxide heterojunction promoted the transfer of photogenerated carriers and inhibited the recombination of electron-hole pairs [73]. In these examples, LDHs/LDOs provides redox pairs or enhances electron separation for catalytic reactions. Combinations with metal-electron rich elements (including metals, tetrathiomolybdc acid, etc.) in LDH materials can significantly improve the catalytic performance. Besides, the presence of metal ions will further affect the overall structure of LDHs/LDOs and bring new active sites, such as oxygen vacancies [74].

2.2.2. Interlayer molecules and anions

Compared to other active sites, interlayer molecules and anions are more active for adsorption and catalysis [58]. Thus, intercalating with various interlayer molecules and anions can obtain multifunctional LDH-based materials. Anions inserted into the LDHs interlayer usually keep their original function. Moreover, as active anions are covered with metal hydroxide layers, the catalytic performance of those modified LDHs is improved and the structure becomes more stable or recyclable [75].

Interlayer ions rely on their own properties to function in the LDH structure. In this respect, Liu et al. prepared a kind of poly-oxonate anion intercalated Tris-LDH- $\text{Zn}_2(\text{PW}_9)_2$, which showed ideal catalytic performance in the cascade reactions with the production of benzyldene ethyl cyanoacetate from benzyl alcohol and ethyl cyanoacetate, and both the activity and selectivity were higher than 99% [76]. Yu et al. synthesized 3D flower-like NiAl-LDH with terephthalic acid (TAL-LDH) and pyromellitic acid (PAL-LDH), then utilized them as an adsorbent for aniline adsorption. Pseudo-second order kinetic model was fitted for both the LDH-based materials, and hydrogen bond between TAL and PAL, π - π interaction, and electrostatic interaction were the major adsorption driving force [77]. Moreover, original LDHs are limited in adsorption of metal ions, thus, intercalated chelators can enhance the ability of LDHs in removing heavy metal ions. According to Pérez et al., EDTA anions were intercalated into ZnAl-LDH to remove metal ions from water without structure

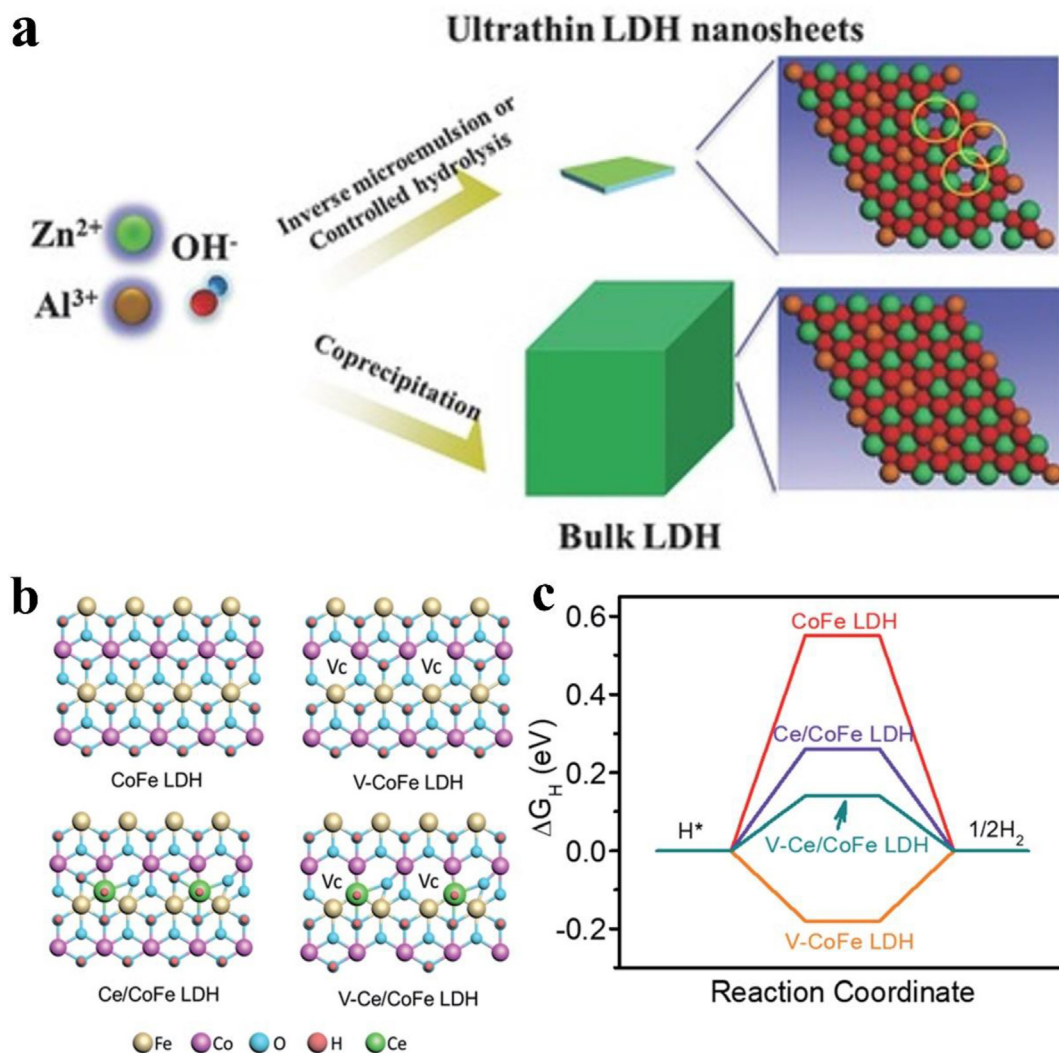


Fig. 3. a) Structure of defects-rich ZnAl-LDH nanosheet [85]; b) Diagram of surface defects on modified CoFe-LDH; c) Comparison of reaction coordinate on the existence of LDH catalyst [103].

destruction and the formed M–EDTA compound was stored in the interlayer structure [75]. The adsorption site was interlayer anion EDTA in similar system [78].

2.2.3. Active structure

The structure of LDH-based materials contains some unique activity, including surface defects, surface charge, pore structure, hydroxide layer, and surface-active groups. In addition to interlayer anions, surface defects are also active sites. Surface defects are potential catalytic sites in developing new high-efficiency catalysts, especially in 2D materials [15,79,80].

Vacancy structures present in LDHs and LDOs. The most common one is oxygen vacancy (O_v). Many oxygen vacancies exist on the metal-rich surface, which changes the surface adsorbed oxygen (O_{ads})/lattice oxygen (O_{latt}) molar ratio. In general, they promote the electron transmission or generation of oxygen radical species [81,82]. With the thinning (*i.e.*, delamination and controllable hydration) of the LDH, vacancies formed [83,84]. An O_v -rich ZnAl-LDH nanosheet showed high ability for CO production according to Zhao et al., the superb catalytic performance was due to the accelerated electron transmission from the oxygen vacancy and strong CO_2 capture ability of Zn-oxygen vacancy complex (Fig. 3a) [85]. Based on electron conduction realized by vacan-

cies electric transition or electric release to h^+ , the conduction ability changed [86]. In another study, series of nanosheets for HER have been developed by Liu et al. (Fig. 3b). Except for active sites provided by metal ions, O_v caused by Ce doping effectively reduced free energy for HER reaction and made it easier to be processed (Fig. 3c) [87]. The doping of polymetallic ions in metal oxide materials effectively enhances the surface energy and oxygen mobility, which means that oxygen vacancy is more easily generated. The conclusion can be demonstrated by density functional theory (DFT) calculations [71,88,89]. According to the study of Zhou et al., the mixed metal oxides caused O_v to add the adsorbed oxygen, which was beneficial for SCR reaction [71]. On the other hand, through vacuum calcination and reduction, modified materials may contain more oxygen vacancies which offer higher catalytic activation compared to ex-LDHs precursors. A ZnCr-LDO calcined in vacuum was utilized for solar photodegradation of bisphenol A. EPR results showed that plenty of oxygen vacancies were formed during vacuum heat treatment and they acted as active sites during photocatalytic reaction [90]. Another available way to induce oxygen vacancy is reduction. Wu et al. reported a vacancy-rich FeCo-LDH produced by H_2 reduction, in which oxygen vacancies dominated the generation of singlet oxygen (1O_2) during SR-AOPs [91].

Metal vacancies can be also introduced into LDHs as active sites. Xie et al. used specific complexing agents to precisely remove Cu from NiCu-LDH, metal vacancy-rich LDHs materials could be used for water splitting [92]. Furthermore, oxygen vacancies and metal vacancies can simultaneously exist on the same LDH. Wang et al. modified NiFe-LDH with methyl-isorhodanate (CH_3NCS). By DFT calculation, they verified that these vacancies could enhance the electroactivity [93].

LDHs also offer positively charged layers as active sites for electric interaction. The hydroxyl groups of LDHs hydroxide layer all point to the interior and the hydroxide layer is positively charged,

leading to that the LDHs have charge compensated an-ion and hydrogen-bonded water [94]. This property determines that the memory effect reconstruction process must be accompanied by the insertion of anions. Meanwhile, the hydroxide layer structure of LDHs exhibits unique activity, which allows for modification, adsorption, and co-catalysis. For example, Zhao et al. reported a LiAl-LDH to remove Cu and Zn through isomorphic substitution. In other words, the adsorption selection of metal ions depended on ionic radii than by the nature of metal ions [95]. The surface groups of LDHs/LDOs also provide activity, Lazaridis et al. utilized the surface precipitation effect caused by the increase of surface

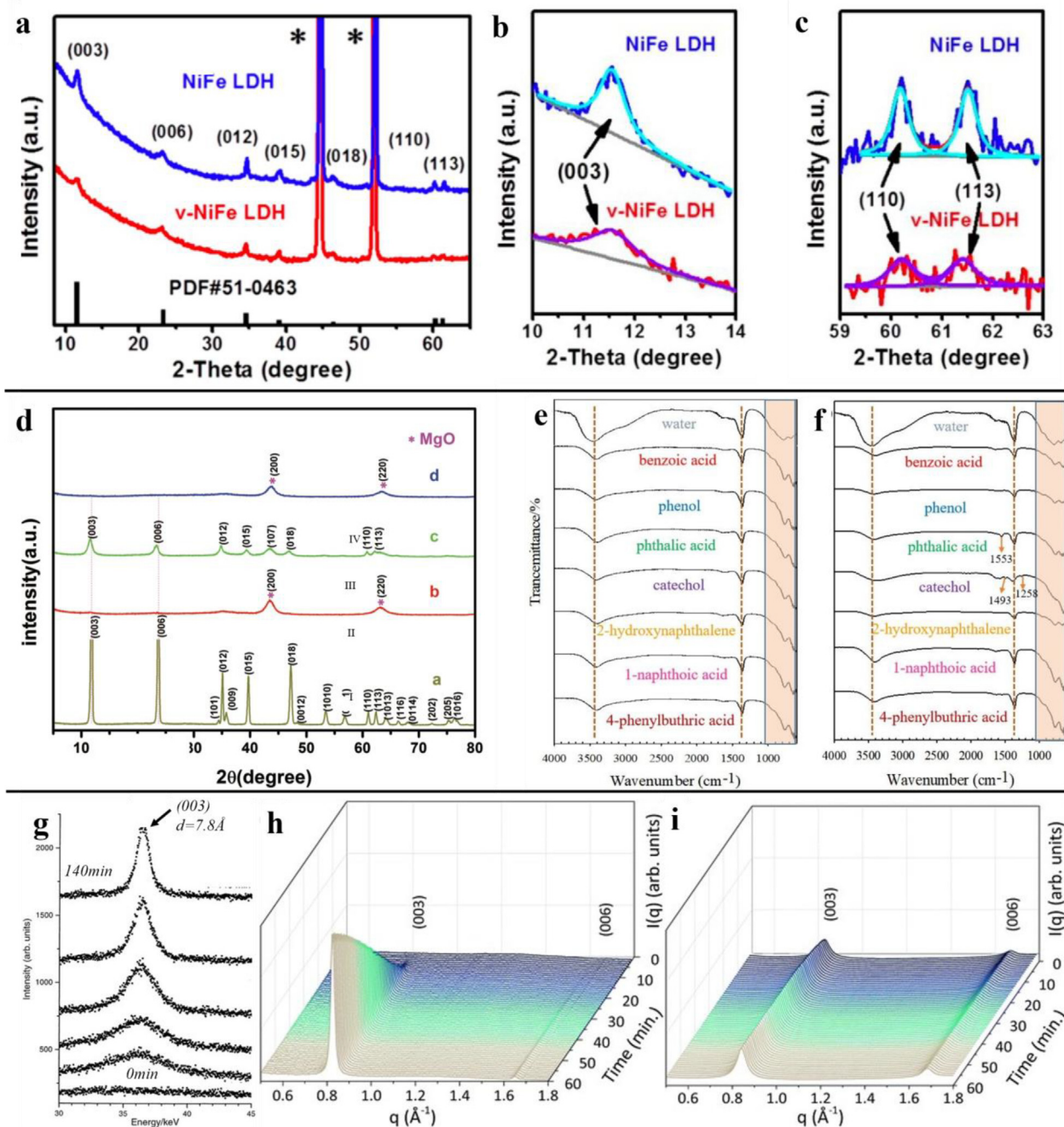


Fig. 4. a) XRD pattern of vacancy-rich LDH; b) The enlargement XRD pattern from Fig. 4a (10–14°), c) The enlargement XRD pattern from Fig. 4a (59–63°) [103], d) XRD peak shifting after loading MnOx(L) LDH, (II) LDO, (III) MnOx-LDH, (IV) MnOx-LDO [105]; e) FT-IR for the regenerated products from Mg-CLDH after 48 h in the presence of modeled aromatic compounds at model concentration: 25 mg/L, f) model concentration: 600 mg/L [108], g) EDXRD spectra measured during the crystallisation of MgAl-LDH from amorphous LDO and sodium carbonate solution at 60 °C at selected times. Each spectrum was acquired in 30 s [106], h) and i) TR-WXAS patterns of LDO reconstruction in water (h) and Acid Blue solution (i) [102].

alkalinity, to further promote the removal of metal ions [96]. Moreover, surface hydroxyl can also be used as a site for loading additional compounds, such as organometallic material, chitosan, and silane to improve the performance [97–99]. At the macro level, the interlayer structure and space originated from loose structure provide sites for adsorption or chelation. A magnetic $\text{Fe}_3\text{O}_4/\text{ZnCr-LDH}$ adsorbent was developed for selective methyl orange (MO) removal from heavy metal wastewater. XRD patterns showed similar layer space before and after adsorption because the adsorption occurred on the surface of transition layer followed by diffusion via the pore structure of LDHs [100].

Therefore, the mechanism of memory effect is a collection of active site behaviors on LDH, such as hydration, surface precipitation, and electrostatic action, which will be described in detail later. In addition, the active site can be retained in the modification process through memory effect (for example, remove some templates by heating), which is similar to the protection of groups in organic synthesis engineering. Other active sites and their properties can be seen as by-products of memory effect.

2.3. A special performance: memory effect

2.3.1. Monitoring of memory effect

The complex mechanism of memory effect makes the reconstructed structure may be different from the ex-LDHs. Understanding the structural changes during the memory effect can help to explain its mechanism and to modify the material for practical applications. With the development of characterization technology, the memory effect can be detected and elucidated at the micro-level. In general, it is necessary to combine multiple characterization approaches to determine the successful synthesis of LDHs with memory effect. This section summarizes some characterization techniques that can be directly used to observe the structural changes of LDH caused by memory effect.

2.3.1.1. In-situ and time-resolved X-ray characterization. X-ray characterization technique can effectively and accurately monitor memory effect. X-ray diffraction (XRD) is a simple and precise method for defining of memory effect. The following properties that may change during memory effect can be determined by XRD: a) surface defects and crystallinity by peak intensity, b) the exchanged intercalation by peak shifting, c) layer spacing by peak position.

Peaks of (00L) [exp. (003), (006), (009)] suggest the existence of LDHs structure, and those peaks will disappear in calcined LDHs [101,102]. According to the XRD pattern (Fig. 4a) from Yuan et al., NiFe-LDH reconstruction in urea solution showed the similarity of re-LDHs and ex-LDHs in characteristic peak [(003), (006), (012), (015)] [103]. XRD peak changed slightly in (003), (110), (113) and the re-LDHs exhibited a weaker peak, indicating the presence of surface oxygen vacancy (Fig. 4b). Furthermore, peak shifting indicates the successful exchange of interlayer anion as well as the layer distance [76,104], which demonstrates the presence of LDHs after ion exchange. Peng et al. utilized potassium permanganate solution as a substrate to reconstruct LDHs from thermal-treated MgAl-LDH. The XRD image of re-LDHs had obvious peak shifting towards a lower degree at (003) and (006), indicating the intercalation of permanganate (Fig. 4c) [105]. The layer space can be determined directly from the position of feature peak of (003) through Bragg's law (Eq. 2-1).

$$2d\sin\theta = n\lambda \quad (2-1)$$

where d is LDH layer space, θ is peak angle, n is diffraction class, and λ is the wavelength of X-Rays.

More recently, time-resolved (TR) X-ray technology can monitor the structures of LDH in real time during memory effect.

Millange et al. utilized time-resolved energy-dispersive X-ray diffraction (TR-EDXRD) in the reconstruction of MgAl-LDO [106]. With the increase of (003) characteristic peak (Fig. 4g), the reformation of LDH structure was confirmed. The dynamic model in the reconstruction process was determined by Avrami-Erofe'ev expression. Time-resolved wide angle X-ray scattering (TR-WAXS) was used to study the mechanism of structural changes during LDH reconstruction [102]. With the rising of (003) peak, the structure of LDH is re-formed and the crystallinity is increasing (Fig. 4h). In addition, the effect of intercalated ions on LDH reconstruction was also observed (Fig. 4i). In addition to using X-rays as a radioactive source, neutron diffraction can also monitor memory effect by chemical bonding behavior, especially the changes of it in water and interlayer anions [107].

2.3.1.2. Microscopy. The microscopic technique can directly show the geometric appearance of LDH material, which can be used to monitor the memory effect. Microscopy including scanning electron microscopy (SEM), transmission electron microscopy (TEM) and atomic force microscope (AFM) can effectively show the geometric properties of LDHs/LDOs.

SEM focuses on the observation of the surface properties of the material. LDH-based materials usually present a flower/nanosheet-like structure in SEM images. By SEM, the range and process of memory effect can be determined. Like XRD pattern, after effective memory effect reconstruction, the crucial character in SEM image is barely changed, re-LDHs still show a nanosheet-like morphology. However, the integrity of the lamellar structure was compromised, which was caused by the presence of defects (Fig. 5a and b) [103]. SEM can be used to speculate the effect of treatment conditions on memory effect. A CoMgAl-LDH was treated in 700 °C and the memory effect was showed in SEM images, the material could be divided into three areas. Memory effect occurs in the region closest to the original material in terms of SEM characteristics (Fig. 5c and 5d) [30]. TEM is more concerned with the inner structure of materials, for LDHs, hexagonal structure and needle-like shape are more common and clearer to measure the reconstruction rates for memory effect according to Xu et al. (Fig. 5e) [108]. Although the layer space could be inferred through XRD, the interlayer spacing, and the layer space changes could be observed by high-resolution transmission electron microscope (HRTEM) due to intercalated ion exchange in a more direct way. AFM can be used to determine the change of crystallinity of LDH materials during memory effect. Daniel et al. used AFM technology to monitor the stearic acid intercalated LDH modified by memory effect and showed that the LDH after reconstruction had lower crystallinity (Fig. 5f and 5g) [109]. Microscopy is the most intuitive way to characterize memory effect. It can make the most accurate judgment on the existence of memory effect, but it is difficult to describe the LDH reconstruction quantitatively like XRD.

2.3.1.3. Fourier transform infrared spectroscopy (FT-IR). The characteristics of chemical groups (such as hydroxyl group), intercalated ions (such as carbonates and nitrates), impurities, and metal oxide particles on the re-LDHs can be determined by FT-IR. Some characteristic peaks have been previously reported (Table 1), which can be used to evaluate the role of memory effect in LDHs reconstruction: a) the existence and ratio of M–O and M–OH to judge the recovery progress, b) interlayer molecules or anions [30,108]. In truth, the corresponding peaks of metal oxides and metal hydroxides are usually a series of peaks in a range. In general, a wavenumber between 900 and 400 cm^{-1} indicates the formation of LDH structure due to the vibrations of M–O and O–M–O structure [110]. Wavenumbers between 3400 and 3600 cm^{-1} and around 1600 cm^{-1} stand for –OH groups. To investigate the influence of humic acid (HA) in memory effect, Xu et al. utilized FT-IR to

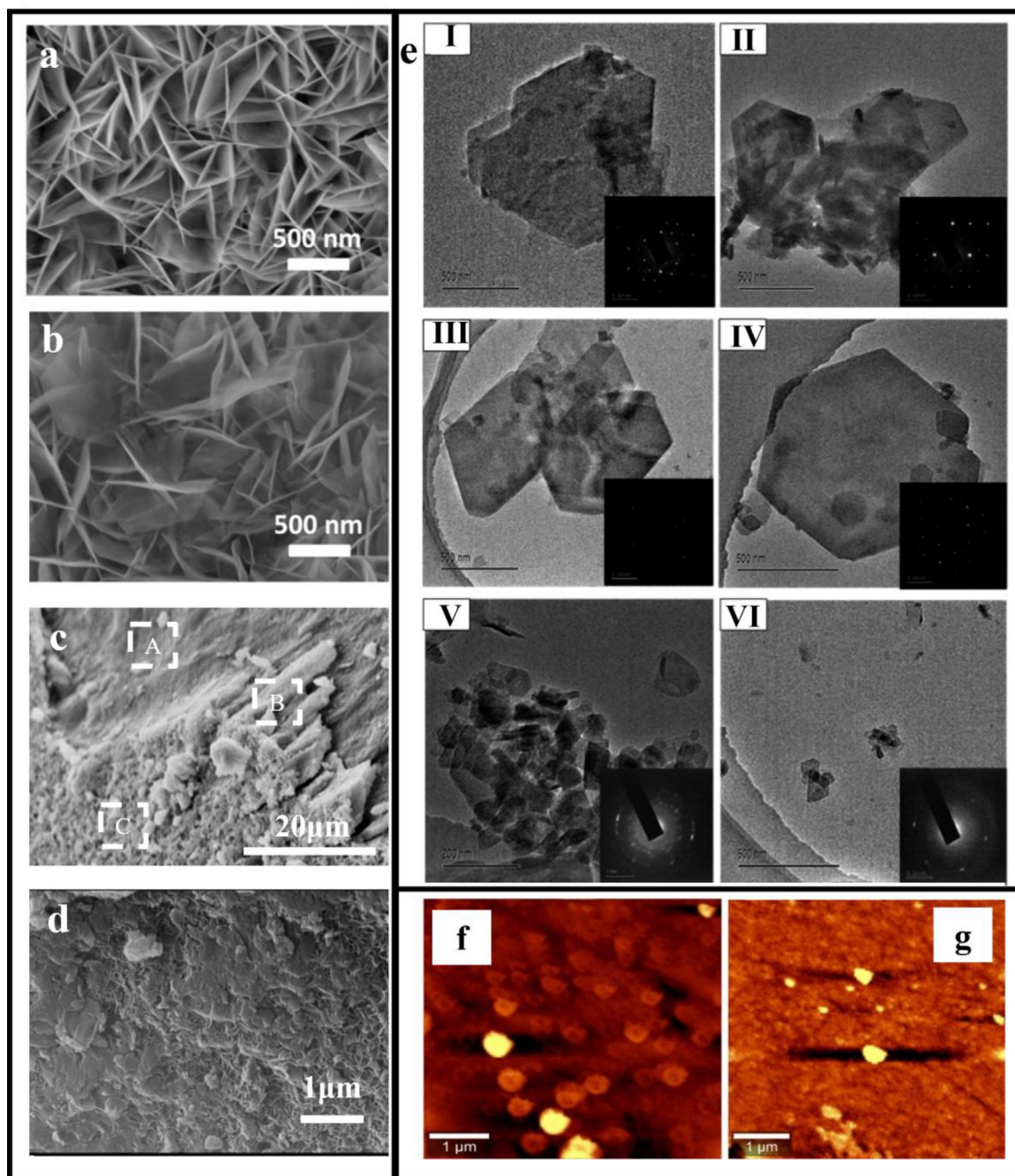


Fig. 5. a) SEM image of ex-NiFe-LDH, b) SEM image of reconstructed defect-rich NiFe-LDH [103], c) Different degrees of recovery on the same LDH. A area: non-reconstruction, B area: broken particles of hydrotalcite support, C area: reconstruction area, d) normal hydrotalcite structure [30], e) TEM image of re-LDHs in various solution [108]. I), II) reconstruction in water; III), IV) reconstruction in phthalic acid, V), VI) reconstruction in catechol, f) & g) AFM image of original and reconstructed LDH [109].

determine the existence of interlayer carbonate, hydroxyl group, benzene ring, and metal-oxide bond in re-LDHs (Fig. 4d and 4e) [108]. For the evaluation of pollutant removal, Guo et al. utilized memory effect as a sorption strategy and the FT-IR results showed the effective removal of acid brown 14 dye and the general existence of hydroxyl bond in LDHs structure, as well as carbonate and water molecules [111].

2.3.1.4. Thermal analysis method. Thermal analysis can be used in LDH calcinating process, which meets the time-resolved monitoring of memory effect. Thermal analysis mainly includes thermogravimetric analysis (TGA), differential scanning calorimetry

(DSC), differential thermal analysis (DTA) in monitoring of memory effect. All thermal analysis results are from the loss of water molecules or interlayer anions during LDO formation. Therefore, thermal analysis can be used to monitor the behavior of materials at different calcination temperatures in memory effect. Thermal analysis can mainly judge the following properties related to memory effect: a) In TGA images, the decomposed components in LDH at this moment can be determined according to the mass loss rate at different stages [109], b) In DSC/DTA images, the evaporation of both water and anion causes a distinct peak [112]. Thermodynamic analysis plays an important role in exploring the key temperature of water and anion evaporation during LDH conversion

Table 1
Wavenumber of LDHs partial structure.

LDH partial structure	Wavenumber cm ⁻¹	Refs.	LDH partial structure	Wavenumber cm ⁻¹	Refs.
Interlayer carbonate	1365	[30]	Adsorbed phosphate	1115	[160]
Interlayer carbonate	1063	[108]	Adsorbed phosphate	945	[160]
Interlayer carbonate	1388	[161]	Adsorbed phosphate	635	[160]
-OH groups	1645	[30]	Adsorbed phosphate	1016	[160]
-OH groups	3600	[30]	Adsorbed phosphate	1090	[44]
-OH groups	3400	[108]	Adsorbed phosphate	1084	[44]
-OH groups	3529	[160]	Mn-OH	864	[162]
-OH groups	3426	[160]	Fe-OH	520	[162]
-OH groups	1612	[160]	Mn-O	607	[162]
-OH groups	1628	[160]	Fe-O	725	[162]
			Co-OH	758	[163]
			Co-O	678	[163]
			Fe-O	518	[163]

to LDO and estimating the influence of temperature on LDH. However, the memory effect recovery process of LDO does not have many advantages. Usually, the mass loss after calcination is compared with standard LDH to determine whether the product of memory effect is really LDH [113].

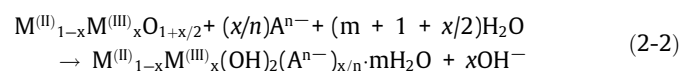
In this section, we discuss some of the techniques that can be used to characterize the memory effect itself. In terms of technical classification, it can be divided into static characterization and dynamic characterization. The object of static characterization is the characterization of LDH before and after memory effect, and LDO products at different calcination temperatures (such as in-situ XRD and microscopy). For dynamic characterization, the entire memory effect process can be monitored by time-resolved technology in real time. The former can help the memory effect to be used in material preparation, such as predicting the catalytic properties of materials or searching for active sites, while the latter is the most convenient means to uncover the mechanism of memory effect. Meanwhile, we summarize some techniques that can be used to characterize LDH: XPS for confirming the existence form of metal ions in LDHs, such as metal valence and oxygen vacancy [114]. BET is another supporter to determine the transformation from LDH to LDO by detailing specific surface area, pore volume, and pore diameter [115]. However, these approaches do not exhibit the unique structure of LDH. XAFS/XANES technology is used to quantitatively determine the oxidation state and coordination status of metal atoms in LDH [116,117]. In fact, time-resolved XAFS and XANES have been well used. Theoretically, they can be used to monitor the changes of metal coordination during the evaporation of LDH to explain the mechanism of memory effect. However, no relevant work has been found using TR-XAFS/XANES techniques. In addition, the time-resolved characterization of LDH memory effect assisted by theoretical chemical computation is becoming mainstream (described in detail below).

2.3.2. Chemical reaction and topological processes: the origin of memory effect

According to the previous works [118,119], the thermal decomposition of LDHs to LDOs suffers 4 steps: a) evaporation of free water, b) loss of intercalated water, c) crystallization of metal oxide, d) decomposition of interlayer anion such as hydroxyl, carbonate, nitrate, phosphate, and structural collapse. And there are two main stages in reconstruction: a) hydration reaction of metal oxides in LDOs, b) re-capture of anions within layer space. However, the mechanism of using hydration reaction of metal oxides to explain memory effect needs further studies. Besides, the more important determinant of memory effect is the evidence of crystal structure in addition to the mechanism of chemical reaction. Much of the controversy surrounding the memory effect stems from the understanding of its chemical reactions. But the more important

question about the memory effect is not how the hydration happens. After the existence of hydration reaction is confirmed (which can be determined by thermodynamics), the change of its topological structure is the basis to fully explain the mechanism of memory effect, and it is also utilized to modify LDH. Therefore, this section will combine evidence from both chemical and topological aspect to explain the memory effect.

Some reports explain memory effect in the view of chemical reactions [37,120]. According to Zhang et al. [36], memory effect was originated from the interaction of multi-metal oxides and H₂O, and finally metal hydroxides were generated to form LDHs structure described as Eq. 2-2.



The general mechanism of memory effect is the “direct synthesis” of multi-metal oxides. Previous reports tried to explain the process by rehydration. MgO and Al₂O₃ were physically mixed to synthesize MgAl-LDH, according to Xu et al. [120]. They demonstrated that hydroxides formed when the metal oxide surfaces were initially hydrated in water. These hydroxides formed in this process showed a sheet-like structure and then adhered to the original oxide surface. Finally, sheet-like hydroxides peeled off to “deposit” in the lattice of another metal oxide, causing the formation of LDH. Meanwhile, a new oxide surface was exposed to make the process continuable. In a report by Gao et al., a calcined MgAl-LDH was reconstructed in water in the same way. However, Zn oxide in calcined ZnAl-LDH would show fewer free states (Zn²⁺) compared with Mg due to the lower hydroxide pKa [6.1 for Zn(OH)₂, 9.5 for Mg(OH)₂], which demonstrates the existence of hydration processes [121]. The direct synthesis mechanism can be used as a component of the mechanism of LDHs memory effect.

In conclusion, without adjusting pH, the chemical mechanism of LDHs recovery is essentially metal dissociation, hydration, nucleation, and agglutination. Ksp or pKa of metal ions has a certain influence on the process, resulting in the difference in LDHs recovery process of different metal composition, though it can be generally explained by the same mechanism [108]. Eq. 2-1 can be divided into the metal release (Eq. 2-3 to 2-4), increasing pH. And then the metal hydroxide is formed (Eq. 2-5 to 2-6), decreasing pH. Finally, hydroxides form layers in specific ways, with water attached (Eq. 2-7). If metal oxide can react with water (such as CaO), the process is more like a one-step process (Eq. 2-8).



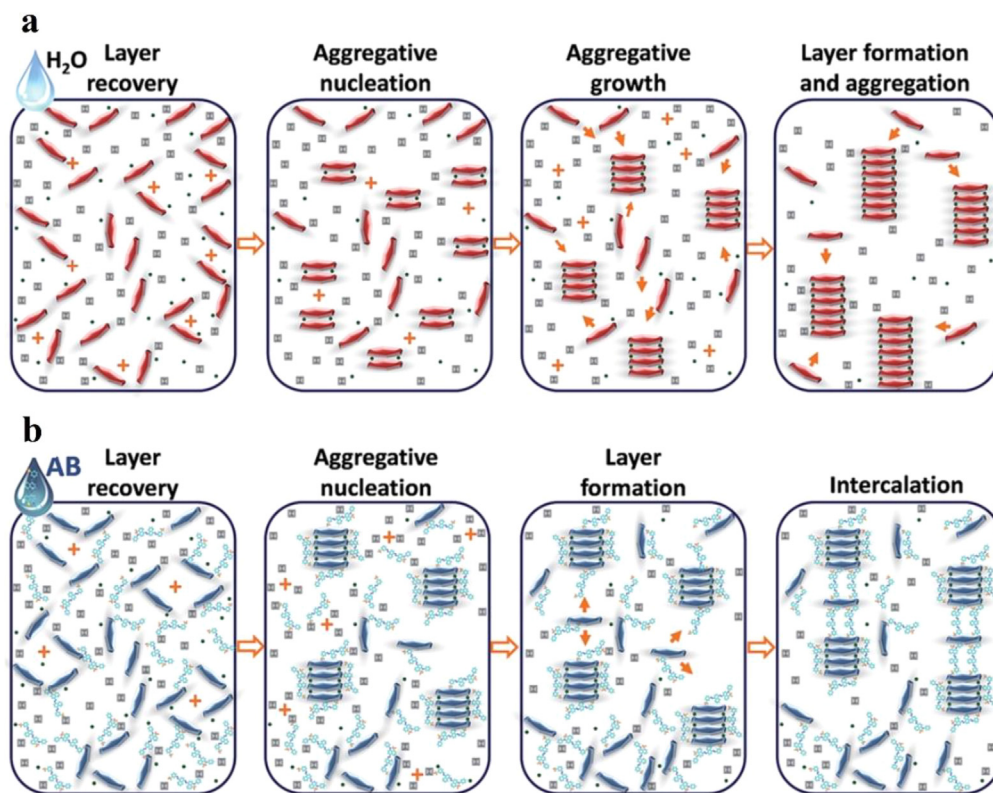
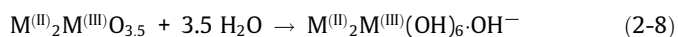
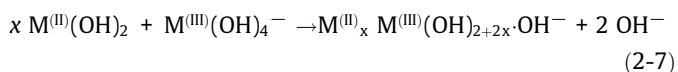


Fig. 6. Topological transition of calcined ZnAl-LDH in a) water and b) Acid blue (AB) 113 azo dye [102].



To the best of our knowledge, the only trivalent metal used in studies of the direct synthesis recovery process is aluminum. However, it can be inferred that most trivalent metals which have memory effect can precipitation and hydration at a relatively low pH like aluminum, the mechanism may still fit for other trivalent metals. Nevertheless, more experiments involving different combinations of metals are needed to reflect the sequence of formation of different hydroxides, which may be related to the number of metal oxides remaining and crystal structure in the final product.

However, the “direct synthesis” is difficult to explain the layered shape on the microtopology. The topological transition may be more important to fully explain the memory effect. In the

XRD pattern, the existence of (003) and (006) crystal face and the increased peak area indicate the successful reconstruction of LDHs structure [122]. Utilization of X-ray absorption spectroscopy (XAS)/wide-angle X-ray scattering (WXAS) to confirm nucleation and aggregative process are steps for reconstruction [102]. Three main processes are related to reconstruction: a) the formation of metal hydroxide nuclei (layered), b) nuclei growing in a direction perpendicular to the layer, and c) the aggregation of nuclei after growth (Fig. 6). This aggregative-growth model contradicts direct synthesis on condensation nuclei. However, if assume that the growth of the layer is to be adsorbed on the surface of the metal oxide, or a hydroxide layer is formed by in-situ hydration of the metal oxide, the contradiction can be explained to some extent. Moreover, the topological mechanism explained from the perspective of layer is far from details to distinguish the relationship between LDHs reconstruction process and the residual structure (it may be non-memory effect metal oxide) after calcinating. Nor can it explain the basis for judging the existence of memory effect.

2.3.3. Thermodynamics and theoretical calculation chemistry: a new horizon for memory effect

Although the traditional studies have explained the memory effect, they have not explained the inevitability of the memory effect and the mechanism of the transformation in a more microscopic structure. More importantly, neither direct synthesis nor lamellar assembly can explain the loss of memory effect of LDO in some cases. The occurrence of LDHs memory effect, especially the surface disintegration of metal oxides and the growth of LDHs nuclei in mechanisms mentioned above, is a process that tends to be thermodynamic stable [102,119]. Thus, based on chemical reactions, there are thermodynamic models used to explain the memory effect recovery of LDHs (Eq. 2-9 and 2-10) [123]. The reaction formula in the previous chemical reaction principle is expressed in the form of Gibbs free energy. This hydration process could be

Table 2

The standard Gibbs free energy for common LDHs metals in hydration reactions [123].

Hydration metal oxide	$\Delta_H G^{\circ} m(298.15 K, M^{m+}(OH)_n)$	Hydration metal oxide	$\Delta_H G^{\circ} m(298.15 K, M^{m+}(OH)_n)$
M^{2+}		M^{3+}	
TiO	33.5	Ga ₂ O ₃	26.2
CuO	12.9	Ti ₂ O ₃	15.9
NiO	11.7	Fe ₂ O ₃	12.1
MnO	1.3	Sb ₂ O ₃	4
ZnO	-0.1	Mn ₂ O ₃	2.1
FeO	-6.6	Al ₂ O ₃	-10
CoO	-8	Ce ₂ O ₃	-59.4
MgO	-26.8		
CaO	-56.2		

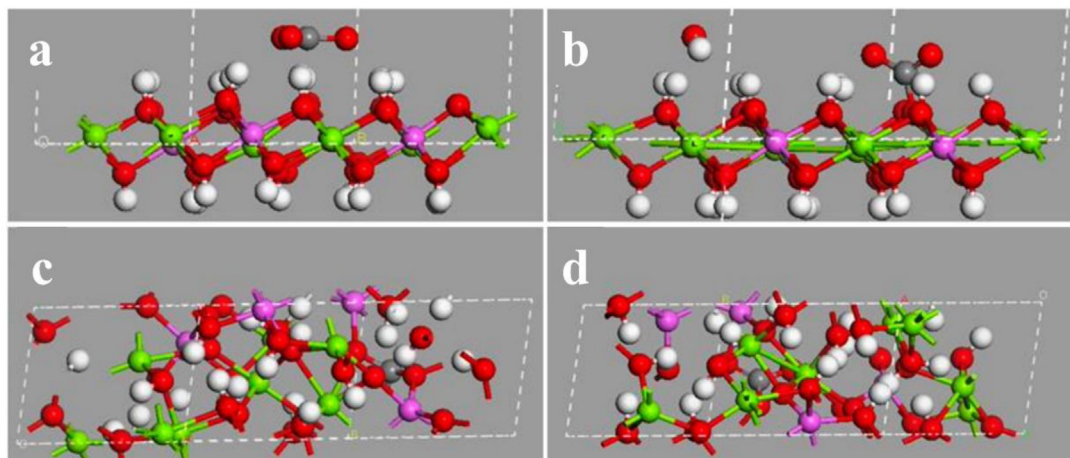
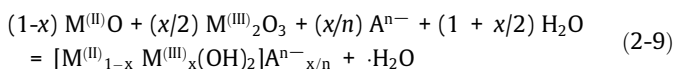


Fig. 7. Snapshots at 30 ps of the NVT (25 °C) dynamic simulations of the CLDH-1 and CLDH-5 structure reconstruction when intercalating. (a) H_2CO_3 and (b) $\text{CO}_2 + \text{H}_2\text{O}$, as well as the memory effect of CLDH-6 by intercalating (c) H_2CO_3 and (d) $\text{CO}_2 + \text{H}_2\text{O}$ [white, H; grey, C; red, O; green, Mg; pink, Al, CLDH-(1-6) means different stage of LDH from calcination beginning to ending] [119].

visualized in molecular dynamics simulations (Eq. 2-11 and 2-12) [124]:



$$\Delta_{\text{HR}} G_{\text{m}}^{\circ}[\text{T}] = (\Delta_{\text{f}} G_{\text{m}}^{\circ}[\text{T}, \text{LDH}] + x \Delta_{\text{f}} G_{\text{m}}^{\circ}[\text{T}, \text{OH}^-]) \\ - ((1-x) \Delta_{\text{f}} G_{\text{m}}^{\circ}[\text{T}, \text{M}^{(II)}\text{O}] + (x/2) \Delta_{\text{f}} G_{\text{m}}^{\circ}[\text{T}, \text{M}^{(III)}_2\text{O}_3] \\ + (x/n) \Delta_{\text{f}} G_{\text{m}}^{\circ}[\text{T}, \text{A}^{n-}] + (1 + x/2) \Delta_{\text{f}} G_{\text{m}}^{\circ}[\text{T}, \text{H}_2\text{O}]) \quad (2-10)$$

$$\Delta_{\text{HR}} G_{\text{m}}^{\circ}[\text{T}, \text{MLC}] = (1-x) \Delta_{\text{H}} G_{\text{m}}^{\circ}[\text{T}, \text{M}^{(II)}\text{O}] + x \Delta_{\text{H}} G_{\text{m}}^{\circ}[\text{T}, \text{M}^{3+}\text{O}] \quad (2-11)$$

$$\Delta_{\text{HR}} G_{\text{m}}^{\circ}[\text{T}, \text{LDH-A}] = (1-x) \Delta_{\text{H}} G_{\text{m}}^{\circ}[\text{T}, \text{M}^{(II)}\text{O}] + x \Delta_{\text{H}} G_{\text{m}}^{\circ}[\text{T}, \text{M}^{(III)}\text{O}] \\ + x \Delta_{\text{C}} G_{\text{m}}^{\circ}[\text{T}, \text{M}^{(II)}\text{A}] \quad (2-12)$$

where MLC denotes LDHs with OH^- intercalation, LDH-A is LDHs with A^{n-} intercalation and A is the intercalation anion (except OH^-).

Combined with the research conclusion of Gibbs free energy, the transition from LDOs to LDHs by memory effect has the thermodynamic spontaneity. Thus, the existence of memory effect can be predicted. The standard Gibbs free energy variation of hydration reaction is summarized, in which no memory effect for the corresponding LDHs of the metal combination satisfies the negative $\Delta_{\text{HR}} G_{\text{m}}^{\circ}$ (Table 2). Use earlier research to test this conclusion: $\text{Mg}_{0.24}\text{Cr}_{0.76}$ -LDO ($\Delta_{\text{HR}} G_{\text{m}}^{\circ} = 22.82$) and $\text{Ni}_{0.81}\text{Al}_{0.19}$ -LDO ($\Delta_{\text{HR}} G_{\text{m}}^{\circ} = 7.577$) failed to reconstruct with positive Gibbs free energy for LDHs generation [125,126]. Therefore, in general, Gibbs free energy can be used to quickly exclude metal combinations without memory effect, which is very effective in the case of a large number of screenings. Despite, Gibbs free energy is available but not the only way to judge memory effect. Memory effect can still occur when reconstructions occurred at higher temperatures. But thermodynamics can only judge the existence of memory effect from an abstract point of view and speculate about the mechanism. The microstructural evidence is the last piece of the puzzle to complete the memory effect.

Th{Zhang, 2016 #18}ermodynamic studies have proved the chemical reaction principle of memory effect in a traditional pathway. Recently, theoretical computational chemistry, such as molecular dynamics simulation, has provided new mechanism evidence for memory effect: the directional transformation of struc-

ture. Zhang et al. utilized molecule simulation to measure the decomposition and reconstruction of LDHs by insertion of water and CO_2 molecules gradually (Fig. 7) [119]. The result showed that the high concentration of O^{2-} in calcined LDHs could adsorb CO_2 into interlayer structure effectively, which explained why CO_3^{2-} intercalation was favorable in topological. Moreover, the memory effect of LDHs is closely related to temperature, and LDOs formed by over-burning (about 800 °C) have an irregular structure instead of the layered structure after the reentry of intercalated ions and loss of active sites (Fig. 7d). Through other simulations, this phenomenon can be attributed to the conversion of the metal oxides (such as MgO and Al_2O_3) formed at the previous temperature from spinel to inverse spinel, which leads to the stagnation of the hydration process. Finally, it causes the disappearance of memory effect and the complete collapse of the layered structure [127,128]. Besides, the loss of water molecules occurs throughout the process: this is consistent with the conversion of hydroxide to oxide. Similarly, for the simulation of the reconstruction process, Meng et al. used a similar method to reconstruct MgFe -LDH and NiAl -LDH [129]. H_2O and CO_2 were inserted into NiAl -CLDH-1 [$\text{Ni}_8\text{Al}_4(-\text{OH})_{18}\cdot 5\text{O}$] and MgFe -CLDH-2 [$\text{Mg}_8\text{Fe}_4(\text{OH})_{16}\cdot 6\text{O}$], which had more complete layered structure, monodentate intermediate was formed and finally converted into LDHs. NiAl -CLDH-2 [$\text{Ni}_8\text{Al}_4(-\text{OH})_{16}\cdot 6\text{O}$] and MgFe -CLDH-3 [$\text{Mg}_8\text{Fe}_4(\text{OH})_{14}\cdot 7\text{O}$] contained higher four-coordinated tetrahedral structure converted from octahedral structure and incomplete layered structure. No symbols about memory effect reconstruction are found in high temperature treated LDOs. Their works provide a new explanation for the topological mechanism of memory effect: calcined-LDH has memory effect on the premise that the layered structure has some integrity in octahedral coordination metal. From this conclusion, it is more reasonable to use LDOs to name calcined LDHs with memory effect.

The thermodynamic instability of LDOs makes it have the tendency of hydration and reconstruction. In terms of chemical reaction, reconstruction is the hydration reaction of two metal oxides to form a hybrid hydroxide process. However, the reconstruction is more reflected in the structure. Firstly, the nucleation and aggregation of hydroxide layers occur in the reconstruction process, which is a structural transformation at the macro level. Secondly, with the help of molecular dynamics simulation, the topological mechanism of memory effect was confirmed: after calcination, the metal coordination structure of LDOs remained consistent with that of LDHs, but too high calcination temperature would destroy this regular eight-ligand structure, and from a macro point of view,

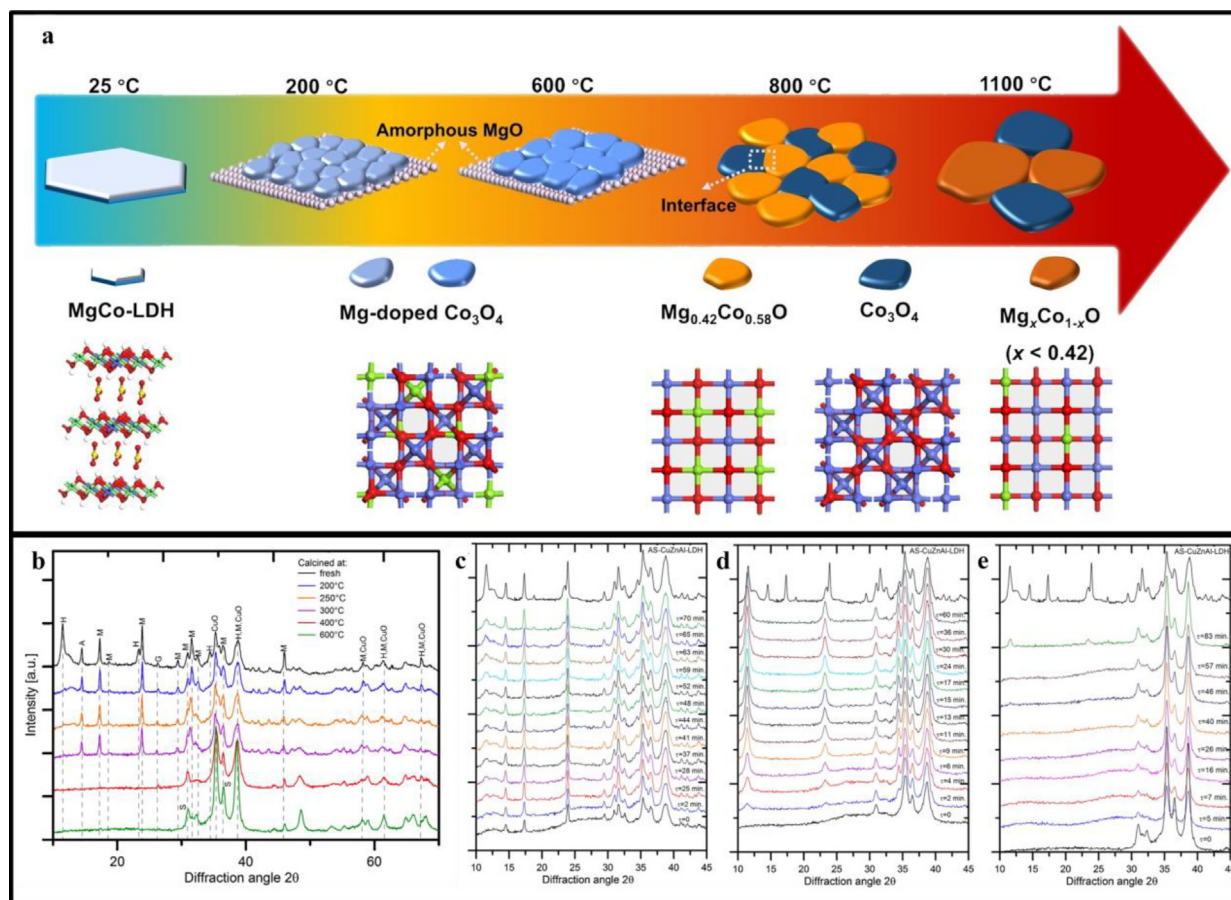


Fig. 8. a) LDH products at different calcination temperatures (MgCo-LDH) [130], b) XRD patterns of AS-CuZnAl-LDH at different temperatures. Only the most prominent peaks are denoted (H—hydratolcite-like Cu-Zn hydroxycarbonate, M—malachite, A—aurichalcite, G—graphite, CuO—copper oxide, S—(Cu_xZn_y)Al₂O₄), c) XRD patterns of the hydration process of CuZnAl-200 °C, d) CuZnAl-400 °C and e) CuZnAl-600 °C [122].

the memory effect disappeared. However, the in-situ hydration resulted from molecular dynamics simulation, which is inconsistent with the conclusions of the hydration, dissociation, and deposition process of bimetal oxides, this inconsistency makes a better amendment to the principle of preparing LDHs by direct synthesis mechanism. The above summary shows that the memory effect and “direct synthesis” are not exactly the same process, they are similar in terms of chemical reaction mechanism and reaction products, but the difference in topology of the reaction process makes them not being simply grouped together.

3. Influence factors of memory effect

The application of memory effect is based on LDHs calcination-reconstruction process, but various conditions may influence the final properties of LDH-based materials. Combined with different modification conditions, re-LDHs can be generated with unique properties compared to ex-LDHs.

3.1. Temperature

Mechanism research has pointed out that calcination temperature makes difference in memory effect. Adjusting calcination temperature is key to generate expected LDH-based materials. This section mainly focuses on the relationship among structure of LDHs/LDOs, memory effect, and calcination process. As concluded, the temperature mainly affects three properties of LDHs/LDOs: a)

structure of formed LDOs, b) existence of memory effect and reconstruction, c) reconstructed structure of re-LDHs. It is interesting that repetitive calcination-hydration also affects the material properties.

Temperature-related properties of LDOs are layer structure, metal oxide amounts, and interlayer molecules, which influence memory effect directly in the structure. Temperature largely determines the type of products and how they behave in terms of memory effect (Fig. 8a) [130]. Kowalik et al. calcined CuZnAl-LDHs at various temperatures. The calcination temperature directly determined the oxide species in products (Fig. 8b-e) [122]. At lower temperature (about 200 °C), the calcined CuZnAl-LDH just lost weak-absorbed water. The appearance of oxide is theoretically impossible. However, due to the limitation of heating conditions, LDH structure is not evenly heated, so local overheating will lead to a very small amount of metal oxide. With the increase of temperature, metal hydroxide or carbonate in the products after treatment was getting lower, and the content of metal oxide was getting higher. Meanwhile, the characteristic peaks of zinc, aluminum oxide, and spinel were not obvious until after 400 °C. Obviously, calcination temperature largely determines the composition of calcination products, higher temperature means higher metal oxide amounts. But the amount of oxide does not determine whether the LDO can be reconstructed. In the reconstruction experiment, C. Gennequin et al. developed a series of partly reconstructive re-LDHs by heating MgAl-LDH in 500, 600, 700, 800, and 900 °C [30]. The specific surface areas of re-LDHs changed in different calcination temperatures. The highest specific surface area (ris-

ing to 214 m²/g from 77 m²/g in original LDHs) was obtained at 500 °C, and with the rising of temperature, decreased specific surface area may be related to the decomposition of layered structure and generation of amorphous phase (only 112 m²/g in 900 °C).

Except that, as mentioned above, high temperature caused the conversion of formed spinel into inverse spinel, bringing the tetrahedral coordination, which could become metal oxide to be loaded on re-LDHs [128]. Extreme temperature can cause the disappearance of memory effect due to too much inverse spinel structure. In another way, the reconstruction speed is also influenced by temperature: calcination in higher temperature offers more rapid reconstruction unexpectedly [122].

3.2. pH

Since the essence of memory is hydration to form hydroxides, pH has a great influence on this process. In fact, according to the reaction mechanism, an increase in pH is a signal for the start of reconstruction. Most of the conclusions on the influence of pH also come from the adsorption experiments of LDOs. Surface charge and hydration processes are also controlled by pH, so they are both discussed here.

Firstly, pH changes the charged state of LDOs surface, which changes the contact between anions and LDOs during the reconstruction process and affects the speed and rates of reconstruction. Under acidic and neutral conditions, many LDOs present protonated surfaces, which have a strong ability to attract anions to intercalate [28,131]. Also, in the case of the synthesis of metal oxides supported-LDHs, pH determines the residual metal oxide. For example, in MgAl-LDO, the changes of pH adjusted the concentration of Mg(OH)₂ and Al(OH)₄⁻. Higher pH led to higher Al(OH)₄⁻ content, which suppressed the hydration of Mg oxide and caused those species to be left in re-LDHs. Conversely, in relatively low pH, more unreacted Al oxide was left [120]. Moreover, under strong acid condition, the formation of metal hydroxide is inhibited, and LDOs will disintegrate and lose the memory effect. However, the effect of pH condition on memory effect is relatively limited compared with other conditions, and the process of LDHs reconstruction is difficult to control pH. Therefore, pH control should not be the first choice to regulate the properties of re-LDHs. However, attention should still be paid to the initial pH when applying the memory effect.

3.3. Metal composition

From the mechanism of memory effect, it can be inferred that the composition of metal elements plays a decisive role in memory effect of LDHs. In the case of memory effect, different metal composition affects the speed and progress of reconstruction, though, the latter is also determined by the burning temperature or controlled by the pH of the oxide residue in the product. The most important reason to think about the different compositions of metal is because it determines whether the memory effect can happen. The existence of memory effect can be judged by Gibbs free energy [124,132].

First, LDHs composed of different metals will present different results when the same calcination condition is performed. Theoretical study of NiAl and MgFe-LDH showed that the latter one was more resistive to high temperature [129]. MgFe-LDH was accompanied by the emergence of the inverse spinel structure later than NiAl-LDH. The critical temperatures of the two LDHs are slightly different. NiAl-LDH lost its carbonate around 365 °C, while MgFe-LDH would not lose carbonate until 380 °C. However, both LDHs lost memory effect in 800 °C. Then related to metal hydration, according to Gao's reports, lower pK_a led to the rapid formation of metal hydroxide reconstruction of re-LDHs, faster reconstruc-

tion of Zn-LDH was achieved compared to Mg-LDH [121]. This significant difference indicated that the composition of different metal layers did influence the memory effect. In addition, the metal ratio in LDHs will also affect the performance of re-LDHs, especially for the occurrence of isomorphous replacement. Wu et al. found that the adsorption capacity of bivalent-cation by calcined LDHs was limited by the half of Mg²⁺ amounts [127], which confirmed that the metal amount in LDH affected the absorption of metal pollutant. During rehydration, isomorphous replacement may lead to heterogeneity in the composition of metal hydroxide layers [133].

3.4. Reconstruction anion and molecules

Temperature, pH, and metal composition is highly relevant to the presence of memory effect, while the anions in the reconstruction medium have a strong influence on the properties of re-LDHs. The interaction among anions, molecules, and LDOs is the most important step in the process of reconstruction. Various anions, including organic and inorganic anions, directly affect the structure, intercalation, and other characteristics of the final product of reconstruction. Moreover, competing intercalation and ion exchange still occur simultaneously during the recovery process, complicating the role of anions in the memory effect.

Firstly, to some extent, the ion radius of intercalated anions determines the layer space of LDHs materials. For every LDHs, whatever is generated by direct synthesis, coprecipitation, ion exchange or reconstruction, those LDHs have the same metal layers and anions [134]. The regulating effect of water molecules on the interlayer structure disables the correlation between the interlayer spacing and the ion radius, corresponding to CaAl-LDH which intercalates with MoS₄²⁻ (Fig. 9a) [17]. Another view is that anions with higher binding capacity (such as carbonate) result in a more stable LDHs structure and smaller LDHs layer region, which will be described in detail in ion competition recovery later [50].

Secondly, the chemical and topological mechanism of memory effect are changed because of the existence of special anions. The most important inorganic anion is carbonate (CO₃²⁻): a) for LDHs, carbonate is the most common intercalated anion, and LDHs synthesized without protective gas is usually carbonate intercalated; b) carbonate as an attacker anion is easy to replace the original anion between the layers of LDHs in an aqueous solution system (Table 3); c) carbonate has the greatest influence on the chemical mechanism of memory effect reconstruction [50,76,129,135]. The existence of carbonate can be used as a model to make it clearer to uncover the process of intercalation. Eq. 2-7 and Eq. 2-8 will be replaced by Eq. 3-1 and Eq. 3-2 after hydration. HA is an important anion affecting the reconstruction of LDHs [112,136,137]. Compared with inorganic anions, HA has obvious and representative effects on re-LDH structure. Xu et al. reported the interaction between LDOs and HAs as normal reconstruction, structure rupture, inhibiting reconstruction and size (Fig. 9b) [108]. All the non-o-benzene HA caused structure rupture in re-LDHs due to the larger electrostatic potential (ESP) than OH⁻ (it means OH⁻ is easier to intercalation) and solubility of metal ion in non-o-benzene (it means the metal-organic complex would be formed). Moreover, there are slightly part of the structure collapse and non-o-benzene intercalation in re-LDHs. All the factors caused the structure-rupture of LDHs. For o-benzene HA, the complex interactions of reconstruction may be due to the presence of metal ions. MgO which was contained in LDO reacted with the added HA firstly, and the further reaction of MgO was suppressed because of the attachment of HA on MgO. When the oxide was CaO, it would prefer to react with water (solvent) directly to form hydroxide. So, HA reacted with Ca hydroxide (Eq. 3-3 and 3-4). However, due to the low ESP of catechol, catechol is quite easy to be adsorbed on

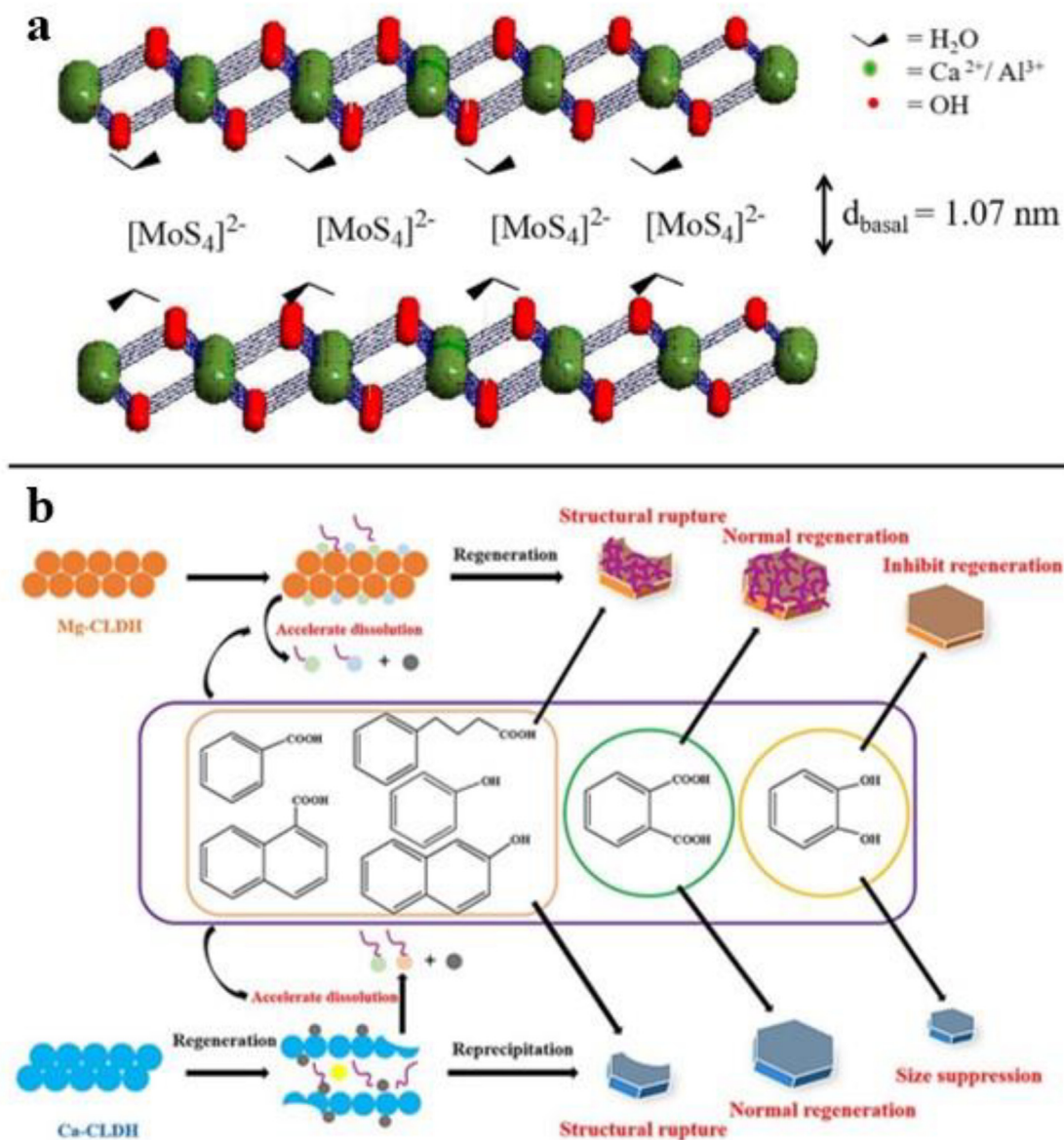


Fig. 9. a) Structure of CaAl-MoS₄-LDH [17], b) reconstruction induced by HA [108].

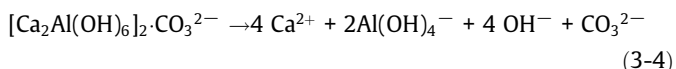
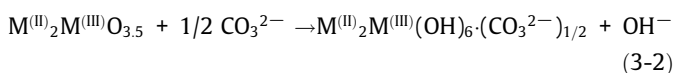
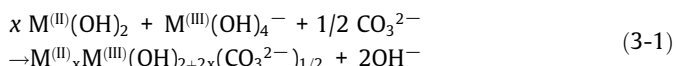
Table 3

Summary of anion competition during LDHs ion exchange and reconstruction.

re-LDHs	Intercalation sequence	Calcination temperature °C	Intercalation method	Refs.
ZnAl-LDH	CO ₃ ²⁻ > OH ⁻ > F ⁻ > Cl ⁻ > Br ⁻ > NO ₃ ⁻	-	Ion exchange	[50]
ZnAl-LDH	PO ₄ ³⁻ > SO ₄ ²⁻	200	Reconstruction	[115]
ZnAl-LDH	HPO ₄ ²⁻ >> SO ₄ ²⁻ > Cl ⁻ , NO ₃ ⁻	200	Reconstruction	[142]
ZnAl-LDH	HPO ₄ ²⁻ >> SO ₄ ²⁻ > Cl ⁻ > NO ₃ ⁻	400	Reconstruction	[142]
ZnAl-LDH	HPO ₄ ²⁻ >> SO ₄ ²⁻ > Cl ⁻ , NO ₃ ⁻	600	Reconstruction	[142]
ZnAl-LDH	HPO ₄ ²⁻ >> Cl ⁻ , NO ₃ ⁻ > SO ₄ ²⁻	800	Reconstruction	[142]
ZnAl-LDH	HPO ₄ ²⁻ >> SO ₄ ²⁻ > Cl ⁻ > NO ₃ ⁻	-	Ion exchange	[142]
ZnAl-LDH	H ₂ PO ₄ ⁻ > CO ₃ ²⁻ > SO ₄ ²⁻ > F ⁻ > NO ₃ ⁻	370	Reconstruction	[112]
MgAl-LDH	erephthalate > 4-methyl-benzoate > benzoate	475	Reconstruction	[134]
MgAl-LDH	OH ⁻ > F ⁻ > Cl ⁻ > Br ⁻ > NO ₃ ⁻ > I ⁻	-	Ion exchange	[135]
MgAl-LDH	CO ₃ ²⁻ > NYS ²⁻ (naphthol yellow S) > SO ₄ ²⁻	-	Reconstruction	[131]
MgAl-LDH	PO ₄ ³⁻ > CO ₃ ²⁻ > SO ₄ ²⁻ > Cl ⁻ > NO ₃ ⁻	500	Reconstruction	[131]
MgAl-LDH	PO ₄ ³⁻ > SCN ⁻	500	Reconstruction	[96]

the metal oxides, which inhibited the hydration of metal oxides and ultimately caused the inhibition of LDH crystal size. The effect of inorganic anions on memory effect has been extensively studied.

The intercalation of inorganic anions has less influence on the morphology and reconstruction of re-LDHs than that of organic anions represented by HA [138].



In the process of LDHs reconstruction, there is an obvious competition between anions, which controls the formation of re-LDHs (Table 3). Due to the positive charge in metal layer, anions are needed when reconstruction. Moreover, positive charge makes anions with more negative charge prior in intercalating. Absorption experiment for LDOs is the efficient way to determine the intercalation sequence. Cardoso et al. dipped a LDO precursor (calcined MgAl-CO₃²⁻ LDH) in mixed organic anion solutions of terephthalate (TA), benzoate (BA) and 4-methyl-benzoate (m-BA), in which the ion valence for TA was -2, and it for mBA and BA was -1 [134]. The adsorption order is TA > mBA > BA. Valence-determined mechanism also is fit for inorganic anions (Table 3). Expect valence, ion radius also determined the intercalation sequence. According to Miyata et al., the dominant intercalated ions have the following characteristics: a) they have smaller radii for ions with same valence properties, and b) they have higher negative valence states for ions with similar radii [135]. In their exchange experiment, monovalent anions are in the sequence of OH⁻ > F⁻ > Cl⁻ > Br⁻ > NO₃⁻ > I⁻, divalent anions are in the sequence of CO₃²⁻ > NYS²⁻ (Naphthol Yellow S) > SO₄²⁻. Similarly, ion exchange sequence of CO₃²⁻ > OH⁻ > F⁻ > Cl⁻ > Br⁻ > NO₃⁻ is also determined by thermodynamic calculation. Phosphate ion has relatively strong intercalation ability due to its -3 valence state. In its presence, other kinds of ions (especially -2 or -1 valence ions) are hard to intercalate. The charge density of host layers, usually determined by rate of M^{(II)I}/M^{(III)I} or M^{(IV)I}, also affects the selective exchange and intercalation. When Mg/Al increases (charge density decreases), the selectivity for SO₄²⁻ and F⁻ decreases, while that for NO₃⁻ increases [52].

Thermodynamics can also account for the existence of ion exchange sequence. As previously described, the hydroxide layer is free during reconstruction, and more systematic studies are needed to explain the competitive role of anions in the reconstruction process. The data obtained from thermodynamic theory shows that the anion with the lowest total energy of LDHs is the most likely to intercalate, which is also in agreement with the experimental results [123,139]. Combined with the study of organic ion intercalation and inorganic ion exchange, some important interactions during LDHs reconstruction can be roughly inferred in a multi-anion system. Therefore, it is correct to think of the order of anion exchange as the order of ion competition during reconstruction. The intercalation by memory effect can avoid the limitation of ion exchange order to a certain extent in the system of single anion. And it is relatively simple in operation.

4. Environmental applications of LDH-based materials with memory effect

LDH-based materials have been widely used in the field of environmental remediation. Adsorption material is the most direct application of memory effect. Although biochar, as a popular material, also has the advantages of simple preparation, flexible regulation, and wide application in environmental remediation, more and more studies have shown that the environmental risks of biochar are real and difficult to estimate [140]. LDH materials that can be completely "artificial" are easier to control environmental risks. Moreover, in recent years, ever more new catalytic materials have been developed to expose, modify, and load catalytic sites by utilizing the memory effect. Remarkably, the memory effect can be used to capture pollutants and catalyze their degradation (Fig. 10).

4.1. Adsorption application

In addition to various adsorption sites in the surface and pore structures, pollutants can also be stored in the recovered layered structures due to the deformation of memory effect [94]. Since reconstruction requires the entry of anions into the interlayer, LDOs with memory effect have a significant adsorption capacity. Theoretically, all anions are capable of being adsorbed through

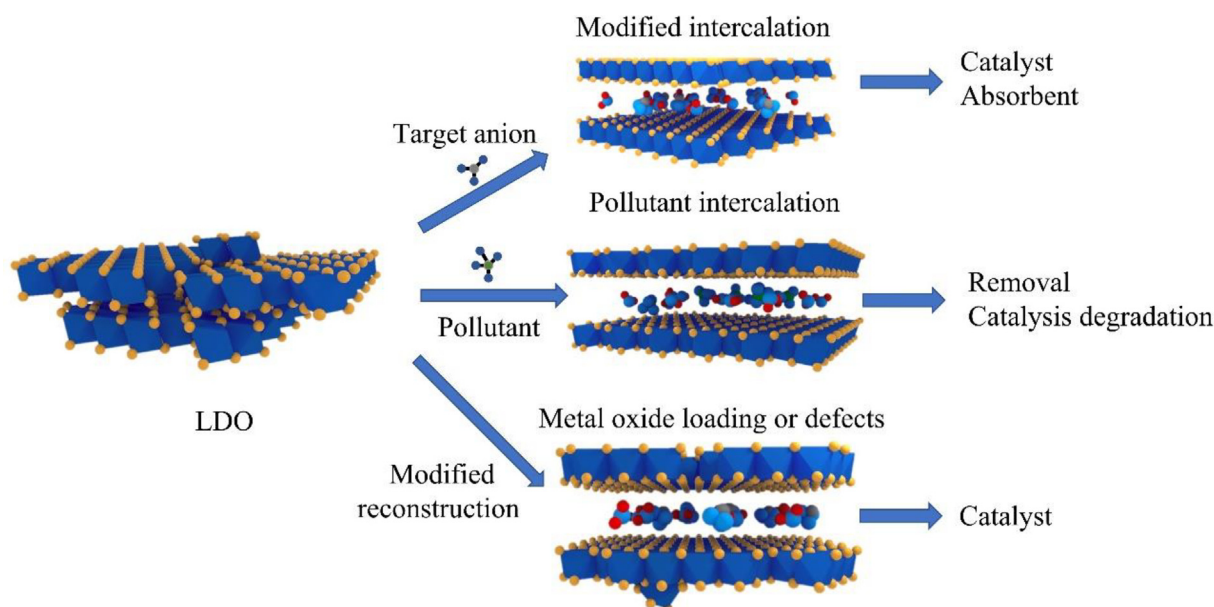


Fig. 10. Main utilization strategies for memory effect LDHs.

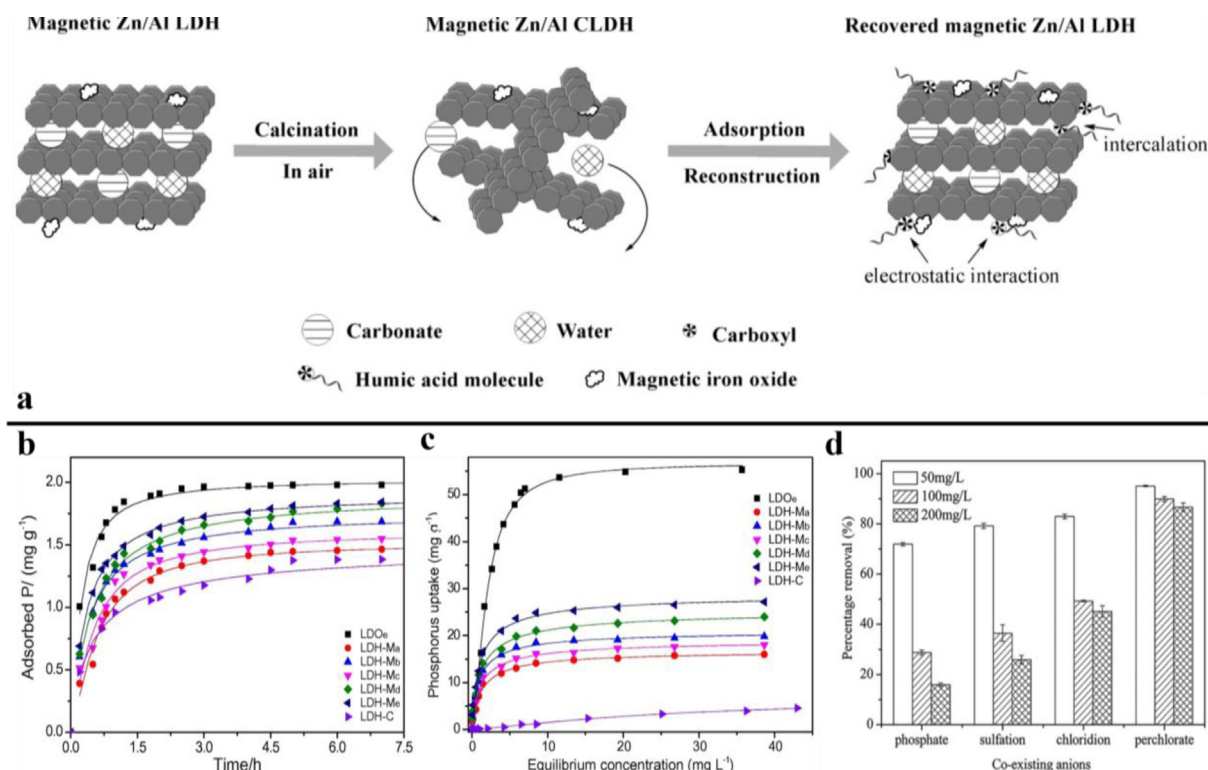


Fig. 11. a) Adsorption mechanism of calcined ZnAl-LDH [112], b) Kinetic study of LDO_e, LDH-M_{a-e} and LDH-C samples at a phosphate concentration of 2 mg/L, c) Phosphate adsorption isotherms of LDO_e, LDH-M_{a-e} and LDH-C samples [144], d) Effect of competitive anions on nitrate adsorption, the initial concentration of nitrate is 100 mg/L [145].

Table 4

Summary of memory effect material as adsorbent.

Materials	Calcination temperature °C	BET surface area m ² /g	Pore volume cm ³ /g	Pollutant	Maximum capacity mg/g	Ref.
Calcined ZnAl-LDO	500	80	0.21	Humic acid	165.84	[112]
ZnAl-LDH	–	49.15	0.18		48.35	[112]
Non-modified MgAl-LDH (LDH-C)	–	53	0.33	Phosphate	1.414	[144]
BMIMP6 and N, N-dimethylformamide modified MgAl-LDH (LDH-Me)	–	291	0.32		1.758	[144]
Calcined LDH-Me (LDO-Me)	500	113	0.46	Nitrate	1.882	[144]
FeMgMn-LDH	–	47.17	–		46.76	[94]
MgAlFe-LDO	450	141.636	–	Nitrate	123.305	[145]
CoFe ₂ O ₄ /MgAl-LDO	450	192.82	0.59	Methyl orange	1219.5	[143]
Magnetic MgAl-LDO/C	500	132.4	0.4285	Cu(II)	386.1 (Cd)	[26]
				Cd(II)	359.7 (Pb)	
				Pb(II)	192.7 (Cu)	
MgAl-LDO	500	–	–	Acid Red G	93.1	[146]
Porous NiLa-LDO/Fe ₃ O ₄	500	97.71	0.35	Phosphate	203.10	[28]
MgFe-LDO	500	78.189	0.45	Perchlorate	27.02	[32]
PdCo-LDO	500	77.232	0.32	Perchlorate	25.32	[32]
Mg _{3.4} Al-LDO	450	–	–	Zn(II)	63.41	[127]
Mg _{3.3} Al-LDO	450	–	–	Zn(II)	402.74	[127]
Mg _{2.9} Al-LDO	450	–	–	Zn(II)	375.28	[127]
ZnAl-LDO	200	85.54	0.178	Phosphate	258.40	[115]
				Sulfate	125.76	[115]
ZnS/Zn-Al LDO	180	58.19	–	Cr(VI)	118.37	[164]

the memory effect. In addition to the memory effect, LDH itself has a certain adsorption capacity by another pathway.

Anion is the most common pollutant that can be adsorbed by LDOs with memory effect. HA plays an important role in the removal of pollutants in water, but it also provides nutrients for the growth of harmful microorganisms, affecting the look and smell of water [141]. Li et al. utilized a ZnAl-LDO as an adsorbent to remove HA and gained 97% removal efficiency in 30 min with

wide pH suitable ranges [112]. In this process, the reconstruction of memory effect is obvious, but the electrostatic adsorption still serves a purpose (Fig. 11a). But the complex organic anions like HA may hinder the recovery process of LDOs. So, most works focused on small inorganic anions. They are also the targets of LDOs adsorption removal by memory effect. For example, He et al. reported a study for the adsorption of phosphate by ZnAl-LDO. When ZnAl-LDH was calcined at a lower temperature, the

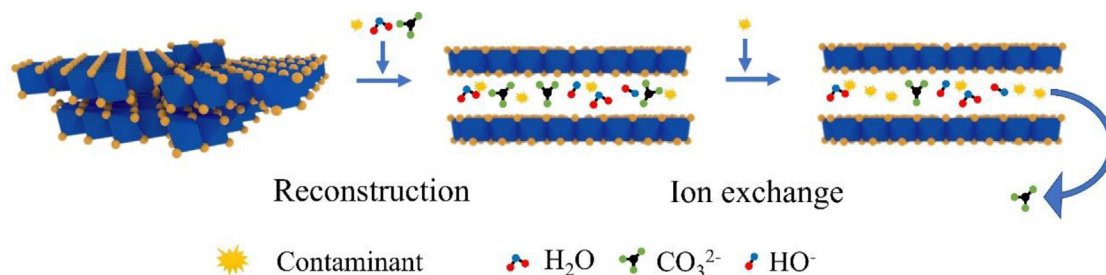


Fig. 12. Two-step adsorption of memory effect.

formed LDOs presented high adsorption capacity, but memory effect was suppressed after calcination at 800 °C, and a sharp drop in adsorption capacity occurred (Table 4). In other studies, when the calcination temperature lower than the temperature which can cause inverse spinel, the LDO products would have higher adsorption efficiency for methyl orange (Table 4) [142,143]. Ultra-thin BMIMPF6 and N, N-dimethylformamide modified LDH (LDH-Me) and calcined production LDO-Me nanosheet materials were used to remove trace phosphate from water. Due to the memory effect, the removal by LDO-Me (94.10 %) was significantly higher than that of LDH-Me (87.90 %), and the adsorption capacity was surprisingly higher than that of non-modified LDH (70.70 %) (Fig. 11b and c, Table 4) [144]. Therefore, based on those examples, memory effect improves the adsorption capacity of LDHs/LDOs materials, especially for anionic pollutants by intercalation. This kind of material for adsorbent has the advantages of easy preparation and low cost. Most LDH can be synthesized by a simple one-pot method (such as urea hydrothermal method) and can be directly roasted to form available LDO adsorbent. By adjusting the roasting temperature, the adsorption performance of LDO can be simply adjusted, which can be rapidly mass-produced in industry. However, there are still some factors that limit its efficiency as adsorbent in some cases.

Despite memory effect shows the strong adsorption ability of various anions in a single anion system, the application of memory effect on adsorption still affected by ion exchange sequence. The existence of competitive ions reduces the adsorption capacity of LDOs materials for target contaminant to some extent [144]. For example, the trivalent electronegativity of phosphate ions makes it easy to be adsorbed by LDOs even in trace (Fig. 12) [143]. The selectivity of memory effect adsorption is based on interlayer electrostatic adsorption, hydrogen bond adsorption, and π - π bond interaction, which limits the adsorption ability of LDOs. The negative effect is more pronounced when in the removal of some less competitive anions like nitrate, which is also a major contributor to eutrophication. For a type of MgAlFe-LDO whose nitrate removal rate can reach 90% in a single system, the adsorption efficiency was inhibited when interference ions are added, especially phosphate [145]. Although the concentration of interfering ions is much higher than the concentration of nitrate (Fig. 11d) and the concentration of phosphate is not so high in most normally produced actual wastewater, the interference of other ions like sulfation and chloridion is a real problem. Another crucial shortcoming is that memory effect-based adsorption materials are not very suitable for recycling. For most reports above, adsorption ability decreases rapidly but is still acceptable after just two or three cycles, especially in recovery by calcination [145,146]. In truth, the recovery method is particularly important. For instance, a NiLa-LDO/Fe₃O₄ still saved its adsorption ability after 7 cycles with the slow-descending adsorption rates by recovery in NaCl solution, but the adsorption might be based on ion exchange [28]. Perhaps

this is related to the uneven local temperature during calcination, resulting in more inverse spinel structures. Also, the decrease of specific surface area and pore volume of LDOs structure affects the adsorption capacity. Therefore, when this kind of material is developed on the premise of recyclability, the combination of LDH metal elements with high temperature resistance should be the first selection. Because ion exchange can still be used as an efficient adsorption mechanism, salt solution also can be chosen as recovery agent.

Although LDOs can reach a high capacity for cation adsorption, memory effect is not an ideal pathway in adsorption of cations, because cations are not attractive for reconstruction. For example, a magnetic MgAl-LDO/C adsorbent gained 98.8%, 96.9%, and 94.6% removal rate for Cu²⁺, Cd²⁺, and Pb²⁺ respectively (Table 4). The adsorption mechanisms were a) surface function adsorption, b) precipitation (to form metal hydroxide or carbonate), and c) electrostatic adsorption, according to Hou et al. [26]. Wu et al. reported that the adsorption of bivalent cation (Me²⁺) by MgAl-LDO was based on the cation exchange and the adsorption capacity of Me²⁺ was limited in half capacity of Mg²⁺ ions, which bond with Al³⁺ in original LDHs (Table 4). Moreover, after adsorption and reconstruction, a MgMeAl-LDH was formed due to the structure rehydration and isomorphic substitution [127]. The adsorption mechanism determined that the removal effect of cations by memory effect was not as effective as that of anion. Hence, more researches are warranted to identify or enhance the advantage of memory effect in cation adsorption.

All the above-mentioned adsorption applications of LDHs are based on “direct removal” of ion intercalation and ion exchange due to the memory effect. However, it is feasible to modify the LDHs with adsorbents intercalation by memory effect. Meanwhile, by comparison, LDOs with memory effect usually have a larger loading capacity than LDHs (Table 4), which means that chelating agents such as EDTA can be used as the active sites to enhance the removal ability of LDH-based materials for heavy metal or other cationic. It also simplifies the procedure of isolating carbonate contamination, which is brought by co-precipitation [43].

In conclusion, the application of memory-effect-based LDH materials in adsorption has been very mature. It has great advantages in the removal of anionic pollutants, especially in the control of water nutrients. For metallic cationic pollutants, memory effect plays a role in adsorption to a certain extent during hydration and precipitation. For other pollutants, the adsorption of memory effect materials is more based on pore structure and electrostatic action, like some mainstream adsorbents such as biochar. However, considering the raw material quality and long-term ecological risk of biochar, it is relatively uncontrollable, especially in persistent free radical or byproduct release, while LDH materials are stable in composition. LDH can avoid most environmental risks through reasonable selection of metal composition, and it may be one of the strong competitors of biochar in adsorption.

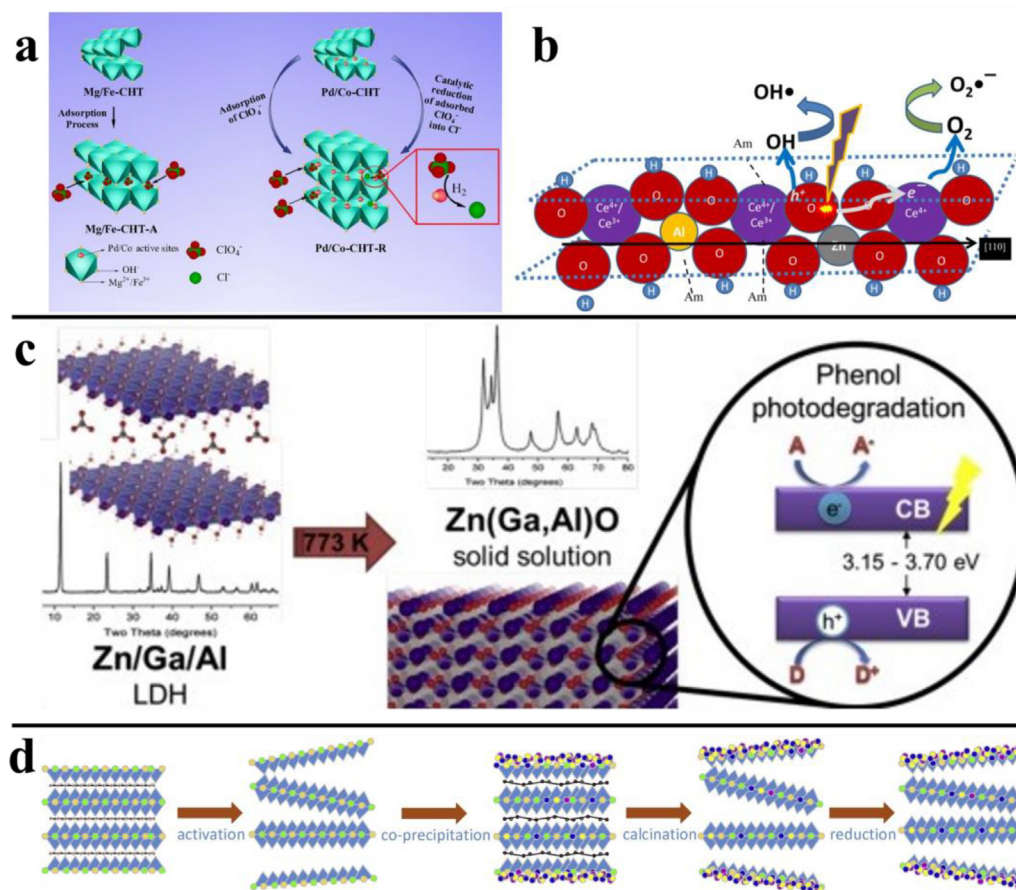


Fig. 13. a) Mechanism of perchlorate removal by MgFe-LDH adsorbent and PdCo-LDH Catalyst [32]; b) Mechanism of interaction between Ce ions, re-LDH and surface hydroxyl [147]; c) Photocatalysis mechanism of ZnGaAl-LDH [151]; d) preparation of Cu-ZnO-ZrO₂-MgAl-LDH by two-step calcination-reconstruction process [153].

Table 5
Summary of memory effect derived re-LDHs catalyst.

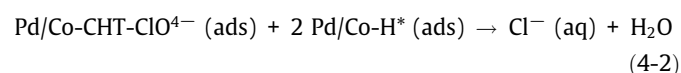
Material	Reaction	Target pollutant	Maximum efficiency %	Activity sites	Refs.
PdCo-LDH	Catalytic hydrogen reduction	Perchlorate 100 ppm	90.9% decontamination	Layer metal	[32]
MnO ₂ /MgAl-LDH	Solvent-free aerobic oxidation	Ethylbenzene 33 mmol/L	5.6% conversion	Loaded Catalyst	[152]
MnO ₂ /MgAl-Si (SH)-LDH	Solvent-free aerobic oxidation	Ethylbenzene 33 mmol/L	29.5% conversion	Loaded Catalyst	[152]
5% Ce/ZnAl-LDH	Photodegradation	Phenol 40 ppm	95% decontamination	Loaded Catalyst	[147]
10% Ce/ZnAl-LDH	Photodegradation	Phenol 40 ppm	82% decontamination	Loaded Catalyst	[147]
3.5% Ce/ZnAl-LDH	Photodegradation	Phenol 40 ppm	81% decontamination	Loaded Catalyst	[147]
ZnAl-LDH	Photodegradation	Phenol 40 ppm	78% decontamination	Layer metal	[147]
ZnAl-LDH	Photodegradation	Phenol 40 ppm	80% decontamination	Layer metal	[151]
ZnGaAl-LDH	Photodegradation	Phenol 80 ppm	60% decontamination	Layer metal	[151]
Cu-ZnO-ZrO ₂ -MgAl-LDH	CO ₂ hydrogenation	CO ₂	78.3% conversion	Loaded Catalyst	[153]
γ -Fe ₂ O ₃ NPs @ Zn ₃ AlFe-LDH	Photodegradation	Phenol 25 ppm	96% decontamination	Loaded Catalyst	[154]
	Photodegradation	4-NP 25 ppm	100% decontamination	Loaded Catalyst	[154]
	Photodegradation	2,4-dinitrophenol 25 ppm	100% decontamination	Loaded Catalyst	[154]
Flower-like ZnS/Zn-Al-LDH	Photoreduction	Cr (IV) 40 mg/L	99.88% Removal	Oxygen Vacancy	[164]

*All the "LDH" means the "reconstructed LDH".

4.2. Catalytic applications

LDHs are considered as perfect catalyst especially for pollutant degradation in electrocatalysis, photocatalysis, and SR-AOPs. Of course, there are some applications in catalytic synthesis or conversion. Environmental catalytic remediation through memory effect-LDHs is mainly carried out through the following ways: a) further catalytic degradation of pollutants after adsorption, b) loading the catalytic site by memory effect while maintaining the structure of LDH. In the first case, the metal elements and LDOs structure can be used as catalytic sites, and the memory effect

promotes the contact between the pollutant and catalyst. MgFe-LDO and PdCo-LDO were compared in perchlorate removal. Though MgFe-LDO had a higher adsorption capacity (Table 4), PdCo-LDO could catalyze hydrogen reduction as Eq. 4-1 and Eq. 4-2. PdCo-LDO gained 90.90% removal efficiency of perchlorate finally [32].



The reaction process is divided into two parts: perchlorate was adsorbed into the interlayer ions through memory effect, and through hydrogen reduction reaction, perchlorate was converted into chloride ions under the catalysis of Pd/Co (Fig. 13a). Moreover, this model also works for organic matter removal. A Ce/ZnAl-LDH was used to adsorb and degrade phenol, and the final decontamination effect had a great relationship with the adsorption performance of the material (Table 5) [147]. This process eliminated the environmental risk of pollutants, compared to simply efficient adsorption. This decontamination strategy maximizes the use of memory effect materials, but there are few practical applications of this strategy.

Modification by memory effect improves the catalytic performance of re-LDHs. Obviously, by the calcination-reconstruction process, more active sites are exposed. The effect of memory effect and carbonate/hydroxide interfering on the catalytic performance of LDHs reconstruction has been studied by cyanoethylation reaction [148]. Re-LDHs show higher acrylonitril conversion than ex-LDHs due to the exposure of O^{2-} and OH^- active sites despite the lower specific surface area. And the isolation of carbonate is the key to rise catalytic ability (Table 4). Re-LDHs catalysts have good photocatalytic properties, especially in inducing the formation of hydroxide radical in reconstruction process [149,150]. LDOs were put in the form of metal oxides and converted into LDHs structure during the reaction process, a large number of hydrogen bond adsorption sites were exposed (Fig. 13b) [147]. Prince et al. utilized a reconstructed ZnAl-LDH and ZnGaAl-LDH for phenol degradation and gained the degradation effect of 80% in 6 h (maximum) (Fig. 13c) [151]. Hydroxyl exchanged carbonate during calcination-reconstruction, which was obvious in 3ZnAl-LDH, gained the highest catalytic ability [151].

Further, the calcination-reconstruction process can be utilized as a method for catalyst loading. For example, a type of LDHs loaded with metal oxides can be synthesized by modulating the memory effect. Lv et al. reported a MnO_2 loaded MgAl-LDHs and gained better conversion rates in ethylbenzene aerobic oxidation. Due to the incomplete reconstruction of memory effect, LDHs catalyst supported by MnO_2 has a lower crystallinity, resulting in a larger specific surface area [152]. MnO_4^{2-} is intercalated in interlayer structure and converted into MnO_2 catalyst, which also fit for AOPs [3]. Due to the surface co-precipitation of LDOs, metal ions can be directly loaded onto LDOs materials and are hydrated together with the memory effect. Meanwhile, they can also be calcined again to be oxidized to form metal oxide catalytic sites. Fang et al. proposed metal oxide loaded by calcination-reconstruction twice (Fig. 13d). And the reconstructed Cu-ZnO-ZrO₂-MgAl-LDH was used for CO₂ hydrogenation and 50% conversion rates were gained, which was higher than the conventional copper catalyst [153]. In the repeated process, the first calcination-reconstruction loaded metal precursors, and the second calcination-reconstruction formed metal oxide on LDHs [153]. A similar process is utilized for the preparation of γ -Fe₂O₃ NPs embedded in ZnAlFe-LDH [154]. The loading of Fe₂O₃ nanoparticles was converted from FeSO₄ on the reconstructed layers. This material gains near-complete decomposition for phenol, 4-NP, and 2,4-dinitrophenol by photocatalytic degradation. Moreover, these LDHs have perfect recycle properties (higher than 90% efficiency after 3 cycles).

Finally, many metals or oxygen vacancies can be formed in LDHs reconstructed by memory effect, which makes it an excellent catalyst. Defects such as oxygen vacancies are often used for advanced oxidation of reactive oxygen species in SR-AOPs. Wu et al. induced oxygen vacancy into Fe₂Co₁-LDH in SR-AOPs as a catalyst for bisphenol A degradation in radical pathway [91]. In general, to obtain sufficient defective sites, memory effect is the more convenient way compared to delamination and reduction methods.

4.3. The suppression of the memory effect

Although memory effect plays a significant role in improving the adsorption capacity of LDOs and catalytic ability of LDHs materials, there are still significant drawbacks of their applications. Unnecessary memory effect prevents materials from working properly in practical applications, which is the main reason to discuss the suppression of the memory effect. Especially, when LDOs are used as catalysts, they must maintain a high specific surface area, pore volume, and eliminate hydrogen bond adsorption, metal hydroxide interference or prevent the influence of CO₂ [132,155]. There are two main methods to suppress the memory effect: a) extreme temperature calcination, b) inhibiting the occurrence of memory effect by co-doping. The former has been described in mechanism, and its effects are evident, while the latter has been less well reported [156]. To promote the catalytic efficiency and material stability, Zhang et al. doped Ce into CoMnAl-LDO (400 °C) by co-precipitation method, which gained perfect stability with the existence of water. Also, the LDOs structure was still kept after NH₃-SCR [157]. Similarly, the addition of Cu may also enhance the resistance of water for MnTi-LDO (400–700 °C) [158]. Limited moisture may help to keep LDOs structure, which is useful in gas adsorption and catalysis [159]. It fundamentally isolates the external conditions for the memory effect to occur. The non-spontaneous hydration reaction of the global LDHs reconstruction reaction (judged by the standard Gibbs free energy) may be an important reason for the inhibition of memory effect [123]. Inhibition of memory effect by composite materials is also a feasible means, but there is no specific study on this strategy at present.

5. Challenges and prospects

As a unique characteristic of LDHs materials, memory effect can be flexibly controlled by calcination temperature, pH, reconstruction, coexisting anions, and metal composition. As a tool for LDH modification, the memory effect has important advantages in the following aspects in real application: a) easy to modify memory effect due to facilitation in calcination construction, b) to enhance catalytic performance by conveniently fabricating LDH materials containing multiple sites (e.g., vacancies, surface hydroxyl groups, and metal oxides), c) to provide high adsorption capacity in the process of structural transformation during reconstruction, especially for anions, d) to enable ion exchange of LDH without NO₃⁻ as an intermediary.

However, in addition to the superior performance of memory effect, there are still some significant deficiencies in the mechanism and application, which prevent the application of memory effect.

(I) Poor cycling performance. In most studies, the memory effect successfully reconstructed the LDHs structure and achieved high efficiency in the initial application process, but the efficiency often declined sharply in the recycling test. It is important to prevent the formation of “inverse spinel” structures during material recovery and calcination, especially for adsorption purposes. Low-temperature and gentle calcination may be the solution while ensuring that the subsequent utilization mechanism remains unchanged, and molecular dynamics simulations have the potential to identify a suitable recovery process.

(II) Limited adsorption. In fact, memory effect-LDOs materials are not suitable for the adsorption of cations. The efficiency and removal rate of surface precipitation and isocrystalline replacement is far less than the ideal of anions. Meanwhile, this exchange may lead to the release of metal ions that constitute LDHs in the water, bringing the risk of secondary pollution. Perhaps the cationic adsorbent intercalated with memory effect is a feasible solution

for the removal of cationic pollution. However, no solution has been proposed for layer ion release, part of the reports referred to an unexpected situation, the co-intercalated of MoS_4^{2-} can adsorb released metal ions, which may solve the isocrystalline replacement contamination [17,48]. Moreover, the memory effect adsorption is very selective for anions, such as phosphate because of the high negative valence and relatively small ion radius. Due to the existence of ion intercalation and exchange sequence in the adsorption of other anions, interference ions can easily affect the removal of target pollutants. More consideration must be given to the nature of the contaminant, such as ionic radius and electrical properties when assessing whether memory effect is applicable or investigating the relationship between ion selectivity and metal composition.

(III) LDHs formed by memory effect have the characteristics of defect structure and metal oxide loading, etc., and those LDHs are an excellent heterogeneous catalyst. However, according to our current statistics, there are few reports on the application of modified LDHs in environmental catalytic remediation, most of which are concentrated in the field of energy like oxidation–reduction reaction and hydrogen reduction reaction. The research of catalysis should jump out of the fixed frame of adsorption–catalysis and the properties of memory effect should be applied to the preparation of the catalyst.

(IV) Limited application in soil or groundwater. Although memory effect-LDOs possess good adsorption properties, the high amount of HA contained in the soil is not conducive to the reconstruction of LDOs in the soil environment and therefore inhibits the adsorption capacity. And there are no relevant reports using memory effect-derived re-LDH as catalyst in soil remediation. To apply memory effect to soil remediation, ex situ remediation (e.g., soil drenching) is more advantageous than in situ remediation, but the cost of the ex-situ remediation is usually more unacceptable. It seems unrealistic to apply memory effect to soils, at least for soil environmental remediation.

Declaration of Competing Interest

The authors declare that they have no known competing financial interests or personal relationships that could have appeared to influence the work reported in this paper.

Acknowledgments

This study was financially supported by the Program for the National Natural Science Foundation of China (51879101, 51579098, 51779090, 51521006, 52100183), the National Program for Support of Top–Notch Young Professionals of China (2014), the Program for Changjiang Scholars and Innovative Research Team in University (IRT-13R17), Hunan Natural Science Foundation (2020JJ3009), Hunan Researcher Award Program (2020RC3025), Hunan Provincial Science and Technology Plan Project (2018SK20410), the Fundamental Research Funds for the Central Universities (531118010473).

References

- [1] A. Karkman, K. Parnanen, D.G.J. Larsson, *Nat. Commun.* 10 (2019) 1–8.
- [2] Y.H. Peng, M.K. Chen, Y.H. Shih, *J. Hazard. Mater.* 260 (2013) 844–850.
- [3] C. Zhang, S. Tian, F. Qin, Y. Yu, D. Huang, A. Duan, C. Zhou, Y. Yang, W. Wang, Y. Zhou, H. Luo, *Water Res.* 194 (2021) 116915.
- [4] R. Karthik, J. Vinoth Kumar, S.M. Chen, C. Karuppiah, Y.H. Cheng, V. Muthuraj, *ACS Appl. Mater. Interfaces* 9 (2017) 6547–6559.
- [5] R.A. Palominos, M.A. Mondaca, A. Giraldo, G. Penuela, M. Perez-Moya, H.D. Mansilla, *Catal. Today* 144 (2009) 100–105.
- [6] S.Y. Liu, C. Lai, B.S. Li, C. Zhang, M.M. Zhang, D.L. Huang, L. Qin, H. Yi, X.G. Liu, F.L. Huang, X.R. Zhou, L. Chen, *Chem. Eng. J.* 384 (2020) 123304.

- [7] Y.K. Fu, G.M. Zeng, C. Lai, D.L. Huang, L. Qin, H. Yi, X.G. Liu, M.M. Zhang, B.S. Li, S.Y. Liu, L. Li, M.F. Li, W.J. Wang, Y.J. Zhang, Z.J. Pi, *Chem. Eng. J.* 399 (2020) 125743.
- [8] M.M. Zhang, C. Lai, B.S. Li, F.H. Xu, D.L. Huang, S.Y. Liu, L. Qin, Y.K. Fu, X.G. Liu, H. Yi, Y.J. Zhang, J.F. He, L. Chen, *Chem. Eng. J.* 396 (2020) 125343.
- [9] B.X. Li, J. He, D.G. Evans, X. Duan, *Appl. Clay Sci.* 27 (2004) 199–207.
- [10] Y. Kuthati, R.K. Kankala, C.H. Lee, *Appl. Clay Sci.* 112 (2015) 100–116.
- [11] S. Samuei, J. Fakkar, Z. Rezvani, A. Shomali, B. Habibi, *Anal. Biochem.* 521 (2017) 31–39.
- [12] L. Cao, J.T. Guo, J.H. Tian, Y. Xu, M.M. Hu, M.Y. Wang, J.J. Fan, *Constr. Build. Mater.* 184 (2018) 203–214.
- [13] C.-W. Chung, H.-Y. Jung, J.-H. Kwon, B.-K. Jang, J.-H. Kim, *J. Struct. Integrity Maint.* 4 (2019) 37–42.
- [14] G. Chen, T. Wang, J. Zhang, P. Liu, H. Sun, X. Zhuang, M. Chen, X. Feng, *Adv. Mater.* 30 (2018) 1706279.
- [15] Y.F. Zhao, X.D. Jia, G.L.N. Waterhouse, L.Z. Wu, C.H. Tung, D. O'Hare, T.R. Zhang, *Adv. Energy Mater.* 6 (2016) 1501974.
- [16] M. Zubair, M. Daud, G. McKay, F. Shehzad, M.A. Al-Harathi, *Appl. Clay Sci.* 143 (2017) 279–292.
- [17] K. Gupta, J.-B. Huo, J.-C.-E. Yang, M.-L. Fu, B. Yuan, Z. Chen, *Chem. Eng. J.* 355 (2019) 637–649.
- [18] A. Jawad, J. Lang, Z.W. Liao, A. Khan, J. Iftikhar, Z.N. Lv, S.J. Long, Z.L. Chen, Z.Q. Chen, *Chem. Eng. J.* 335 (2018) 548–559.
- [19] G. Fan, F. Li, D.G. Evans, X. Duan, *Chem. Soc. Rev.* 43 (2014) 7040–7066.
- [20] R.N. Guo, L.C. Nengzi, Y. Chen, Y.H. Li, X.Y. Zhang, X.W. Cheng, *Chem. Eng. J.* 398 (2020) 125676.
- [21] R. Ramachandran, S. Thangavel, L. Minzhang, S. Haiquan, X. Zong-Xiang, F. Wang, *Chemosphere* 271 (2021) 128509.
- [22] J.W. Zhao, J. Chen, S.M. Xu, M.F. Shao, Q. Zhang, F. Wei, J. Ma, M. Wei, D.G. Evans, X. Duan, *Adv. Funct. Mater.* 24 (2014) 2938–2946.
- [23] H. Chen, L.F. Hu, M. Chen, Y. Yan, L.M. Wu, *Adv. Funct. Mater.* 24 (2014) 934–942.
- [24] X.R. Zhou, Z.T. Zeng, G.M. Zeng, C. Lai, R. Xiao, S.Y. Liu, D.L. Huang, L. Qin, X.G. Liu, B.S. Li, H. Yi, Y.K. Fu, L. Li, Z.H. Wang, *Chem. Eng. J.* 383 (2020) 123091.
- [25] W. Zou, W. Guo, X. Liu, Y. Luo, Q. Ye, X. Xu, F. Wang, *Chemistry* 24 (2018) 19309–19316.
- [26] T.L. Hou, L.G. Yan, J. Li, Y.T. Yang, L.X. Shan, X. Meng, X.G. Li, Y.X. Zhao, *Chem. Eng. J.* 384 (2020) 123331.
- [27] N. Nityashree, P. Menezes, *Appl. Nanosci.* 3 (2013) 321–327.
- [28] C.T. Vu, T. Wu, *Water Res.* 175 (2020) 115679.
- [29] T.S. Xue, R.N. Li, Y.S. Gao, Q. Wang, *Chem. Eng. J.* 384 (2020) 123284.
- [30] C. Gennequin, T. Barakat, H.L. Tidahy, R. Cousin, J.F. Lamonier, A. Aboukais, S. Siffert, *Catal. Today* 157 (2010) 191–197.
- [31] Y. Chen, J.C. Yan, D. Ouyang, L.B. Qian, L. Han, M.F. Chen, *Appl. Catal. A- General* 538 (2017) 19–26.
- [32] Y.D. Liu, Y. Liu, Q.C. He, P.L. Guo, J. Chen, D.J. Wan, S.H. Xiao, *Colloids Surf. A- Physicochem. Eng. Aspects* 593 (2020) 124641.
- [33] Z.Z. Yang, J.J. Wei, G.M. Zeng, H.Q. Zhang, X.F. Tan, C. Ma, X.C. Li, Z.H. Li, C. Zhang, *Coord. Chem. Rev.* 386 (2019) 154–182.
- [34] Z.Z. Yang, F.H. Wang, C. Zhang, G.M. Zeng, X.F. Tan, Z.G. Yu, Y. Zhong, H. Wang, F. Cui, *RSC Adv.* 6 (2016) 79415–79436.
- [35] Q. Yan, X. Hou, G. Liu, Y. Li, T. Zhu, Y. Xin, Q. Wang, *J. Hazard. Mater.* 400 (2020) 123260.
- [36] G.H. Zhang, X.Q. Zhang, Y. Meng, G.X. Pan, Z.M. Ni, S.J. Xia, *Chem. Eng. J.* 392 (2020) 123684.
- [37] G. Mascolo, C.M. Mascolo, *Microporous Mesoporous Mater.* 214 (2015) 246–248.
- [38] A. Malak-Polaczyk, C. Vix-Guterl, E. Frackowiak, *Energy Fuels* 24 (2010) 3346–3351.
- [39] J.D. Hong, W. Zhang, Y.B. Wang, T.H. Zhou, R. Xu, *ChemCatChem* 6 (2014) 2315–2321.
- [40] R. Yang, Y.M. Zhou, Y.Y. Xing, D. Li, D.L. Jiang, M. Chen, W.D. Shi, S.Q. Yuan, *Appl. Catal. B- Environ.* 253 (2019) 131–139.
- [41] S.O. Ganiyu, T.X.H. Le, M. Bechelany, G. Esposito, E.D. van Hullebusch, M.A. Oturan, M. Cretin, *J. Mater. Chem. A* 5 (2017) 3655–3666.
- [42] Y. Liu, Q.Q. Xiong, H.W. Song, Y.X. Peng, L. Liu, C.W. Jiang, *Cellulose* 26 (2019) 2573–2585.
- [43] H. Chen, J. Lin, N. Zhang, L. Chen, S. Zhong, Y. Wang, W. Zhang, Q. Ling, *J. Hazard. Mater.* 345 (2018) 1–9.
- [44] Z. Zhang, L. Yan, H. Yu, T. Yan, X. Li, *Bioresour. Technol.* 284 (2019) 65–71.
- [45] P. Gunawan, R. Xu, *Chem. Mater.* 21 (2009) 781–783.
- [46] E.M. Seftel, M.C. Puscasu, M. Mertens, P. Cool, G. Carja, *Appl. Catal. B- Environ.* 164 (2015) 251–260.
- [47] E.M. Seftel, M.C. Puscasu, M. Mertens, P. Cool, G. Carja, *Appl. Catal. B- Environ.* 150 (2014) 157–166.
- [48] J. Ali, L. Wenli, A. Shahzad, J. Iftikhar, G.G. Aregay, Z. Shahib II, Z. Elkhilifi, Z.C. Chen, *Water Res.* 181 (2020) 115862.
- [49] J. Das, B.S. Patra, N. Baliarsingh, K.M. Parida, *Appl. Clay Sci.* 32 (2006) 252–260.
- [50] D.G. Costa, A.B. Rocha, W.F. Souza, S.S.X. Chiaro, A.A. Leitão, *Appl. Clay Sci.* 56 (2012) 16–22.
- [51] H.W. Olfis, L.O. Torres-Dorante, R. Eckelt, H. Kosslick, *Appl. Clay Sci.* 43 (2009) 459–464.
- [52] T. Hibino, *Eur. J. Inorg. Chem.* 2018 (2018) 722–730.
- [53] T. Hibino, M. Kobayashi, *J. Mater. Chem.* 15 (2005) 653–656.
- [54] J. Wang, W. Bao, A. Umar, Q. Wang, D. O'Hare, Y. Wan, *J. Biomed. Nanotechnol.* 12 (2016) 922–933.

- [55] T. Kameda, D. Ikeda, S. Kumagai, Y. Saito, T. Yoshioka, *Inorg. Chem. Commun.* 122 (2020) 108266.
- [56] K. Cermelj, K. Ruengskajorn, J.C. Buffet, D. O'Hare, *J. Energy Chem.* 35 (2019) 88–94.
- [57] L. Tian, H. Xiaojie, B. Sha, Z. Yufei, S. Yu-Fei, *Acta Phys. Chim. Sin.* 36 (2020) 1912005.
- [58] Y.N. Sun, B. Gao, Y. Yao, J.N. Fang, M. Zhang, Y.M. Zhou, H. Chen, L.Y. Yang, *Chem. Eng. J.* 240 (2014) 574–578.
- [59] J. He, C. Lai, L. Qin, B. Li, S. Liu, L. Jiao, Y. Fu, D. Huang, L. Li, M. Zhang, X. Liu, H. Yi, L. Chen, Z. Li, *Chemosphere* 256 (2020) 127083.
- [60] C. Lai, F. Xu, M. Zhang, B. Li, S. Liu, H. Yi, L. Li, L. Qin, X. Liu, Y. Fu, N. An, H. Yang, X. Huo, X. Yang, H. Yan, *J. Colloid Interface Sci.* 588 (2021) 283–294.
- [61] L. Qin, Z. Wang, Y. Fu, C. Lai, X. Liu, B. Li, S. Liu, H. Yi, L. Li, M. Zhang, Z. Li, W. Cao, Q. Niu, *J. Hazard. Mater.* 414 (2021) 125448.
- [62] M. Zhang, C. Lai, B. Li, F. Xu, D. Huang, S. Liu, L. Qin, X. Liu, H. Yi, Y. Fu, L. Li, N. An, L. Chen, *Chem. Eng. J.* 422 (2021) 130120.
- [63] M.Y. Gao, X.W. Chen, W.X. Huang, L. Wu, Z.S. Yu, L. Xiang, C.H. Mo, Y.W. Li, Q. Y. Cai, M.H. Wong, H. Li, *J. Hazard. Mater.* 416 (2021) 125894.
- [64] H.T. Lu, M.H. Sui, B.J. Yuan, J.Y. Wang, Y.N. Lv, *Chem. Eng. J.* 357 (2019) 140–149.
- [65] R. Guo, Y. Li, Y. Chen, Y. Liu, B. Niu, J. Gou, X. Cheng, *Chem. Eng. J.* 417 (2021) 127887.
- [66] Z. Li, Y. Sun, Y. Yang, Y. Han, T. Wang, J. Chen, D.C.W. Tsang, *J. Hazard. Mater.* 383 (2020) 121240.
- [67] C.A. Antonyraj, S. Kannan, *Appl. Clay Sci.* 53 (2011) 297–304.
- [68] Y. Yao, Y. Cai, G. Wu, F. Wei, X. Li, H. Chen, S. Wang, *J. Hazard. Mater.* 296 (2015) 128–137.
- [69] Y. Zhang, Q. Zhang, Z. Dong, L. Wu, J. Hong, *Water Res.* 146 (2018) 232–243.
- [70] Y.C. Hong, H.Y. Zhou, Z.K. Xiong, Y. Liu, G. Yao, B. Lai, *Chem. Eng. J.* 391 (2020) 123604.
- [71] X. Zhou, F. Yu, R.B. Sun, J.Q. Tian, Q. Wang, B. Dai, J.M. Dan, H. Pfeiffer, *Appl. Catal. A-General* 592 (2020) 117432.
- [72] S.H. Begum, C.T. Hung, Y.T. Chen, S.J. Huang, P.H. Wu, X.X. Han, S.B. Liu, *J. Mol. Catal. A-Chem.* 423 (2016) 423–432.
- [73] X.X. Liu, Q. Shao, Y.F. Zhang, X.J. Wang, J. Lin, Y.F. Gan, M.Y. Dong, Z.H. Guo, *Colloids Surf. A-Physicochem. Eng. Aspects* 592 (2020) 124588.
- [74] L.Y. Chen, Y.Y. Zhang, D.Z. Li, Y.X. Wang, C.Y. Duan, *J. Mater. Chem. A* 6 (2018) 18378–18383.
- [75] M.R. Pérez, I. Pavlovic, C. Barriga, J. Cornejo, M.C. Herminos, M.A. Ulibarri, *Appl. Clay Sci.* 32 (2006) 245–251.
- [76] K. Liu, Y.Q. Xu, Z.X. Yao, H.N. Miras, Y.F. Song, *ChemCatChem* 8 (2016) 929–937.
- [77] S. Yu, X. Wang, Z. Chen, J. Wang, S. Wang, T. Hayat, X. Wang, *J. Hazard. Mater.* 321 (2017) 111–120.
- [78] R. Rojas, M.R. Perez, E.M. Erro, P.I. Ortiz, M.A. Ulibarri, C.E. Giacomelli, *J. Colloid Interface Sci.* 331 (2009) 425–431.
- [79] J. Xiong, J. Di, J.X. Xia, W.S. Zhu, H.M. Li, *Adv. Funct. Mater.* 28 (2018) 1801983.
- [80] X.Q. Huo, Y. Yang, Q.Y. Niu, Y. Zhu, G.M. Zeng, C. Lai, H. Yi, M.F. Li, Z.W. An, D.L. Huang, Y.K. Fu, B.S. Li, L. Li, M.M. Zhang, *Chem. Eng. J.* 403 (2021) 126363.
- [81] S. Mo, S. Li, J. Li, Y. Deng, S. Peng, J. Chen, Y. Chen, *Nanoscale* 8 (2016) 15763–15773.
- [82] Z. Wu, M. Li, J. Howe, H.M. Meyer 3rd, S.H. Overbury, *Langmuir* 26 (2010) 16595–16606.
- [83] M. Xu, M. Wei, *Adv. Funct. Mater.* 28 (2018) 1802943.
- [84] Q. Wang, Z.Q. Liu, D.M. Liu, G.S. Liu, M. Yang, F.Y. Cui, W. Wang, *Appl. Catal. B-Environ.* 236 (2018) 222–232.
- [85] Y. Zhao, G. Chen, T. Bian, C. Zhou, G.I. Waterhouse, L.Z. Wu, C.H. Tung, L.J. Smith, D. O'Hare, *T. Zhang, Adv. Mater.* 27 (2015) 7824–7831.
- [86] Y. Shin, K.-Y. Doh, S.H. Kim, J.H. Lee, H. Bae, S.-J. Song, D. Lee, *J. Mater. Chem. A* 8 (2020) 4784–4789.
- [87] S.J. Liu, J. Zhu, M. Sun, Z.X. Ma, K. Hu, T. Nakajima, X.H. Liu, P. Schmuki, L. Wang, *J. Mater. Chem. A* 8 (2020) 2490–2497.
- [88] S. Rong, P. Zhang, F. Liu, Y. Yang, *ACS Catal.* 8 (2018) 3435–3446.
- [89] S.N. Chen, Q.H. Yan, C. Zhang, Q. Wang, *Catal. Today* 327 (2019) 81–89.
- [90] M.Q. Chen, P.X. Wu, Q.Q. Wei, Y.J. Zhu, S.S. Yang, L.T. Ju, N.W. Zhu, Z. Lin, *Environ. Chem.* 15 (2018) 226–235.
- [91] L.Y. Wu, J.M. Hong, Q. Zhang, B.Y. Chen, J. Wang, Z.Y. Dong, *Chem. Eng. J.* 385 (2020) 123620.
- [92] Y.S. Xie, Z. Wang, M. Ju, X. Long, S. Yang, *Chem. Sci.* 10 (2019) 8354–8359.
- [93] Y.Q. Wang, S. Tao, H. Lin, G.P. Wang, K.N. Zhao, R.M. Cai, K.W. Tao, C.X. Zhang, M.Z. Sun, J. Hu, B.L. Huang, S.H. Yang, *Nano Energy* 81 (2021) 105606.
- [94] H. Zhou, Y. Tan, W. Gao, Y. Zhang, Y. Yang, *Sci. Rep.* 10 (2020) 16126.
- [95] L.X. Zhao, J.L. Liang, N. Li, H. Xiao, L.Z. Chen, R.S. Zhao, *Sci. Total Environ.* 716 (2020) 137120.
- [96] N.K. Lazaridis, *Water Air Soil Pollut.* 146 (2003) 127–139.
- [97] F. Lyu, H. Yu, T. Hou, L. Yan, X. Zhang, B. Du, *J. Colloid Interface Sci.* 539 (2019) 184–193.
- [98] C.M.R. Wright, K. Ruengskajorn, A.F.R. Kilpatrick, J.C. Buffet, D. O'Hare, *Inorg. Chem.* 56 (2017) 7842–7850.
- [99] C. Chen, J.C. Buffet, D. O'Hare, *Dalton Trans.* 49 (2020) 8498–8503.
- [100] D. Chen, Y. Li, J. Zhang, W. Li, J. Zhou, L. Shao, G. Qian, *J. Hazard. Mater.* 243 (2012) 152–160.
- [101] P. Kowalik, M. Konkol, M. Kondracka, W. Próchniak, R. Bicki, P. Wiercioch, *Appl. Catal. A* 464–465 (2013) 339–347.
- [102] R.M.M. Santos, J. Tronto, V. Briois, C.V. Santilli, *J. Mater. Chem. A* 5 (2017) 9998–10009.
- [103] Z.J. Yuan, S.M. Bak, P.S. Li, Y. Jia, L.R. Zheng, Y. Zhou, L. Bai, E.Y. Hu, X.Q. Yang, Z. Cai, Y.M. Sun, X.M. Sun, *ACS Energy Lett.* 4 (2019) 1412–1418.
- [104] T. Bujdosó, Á. Patzkó, Z. Galbács, I. Dékány, *Appl. Clay Sci.* 44 (2009) 75–82.
- [105] H.H. Peng, J. Chen, Y. Jiang, de, X.L. Guo, H. Chen, Y.X. Zhang, *Dalton Trans.*, 45 (2016) 10530–10538.
- [106] F. Millange, R.I. Walton, D. O'Hare, *J. Mater. Chem.* 10 (2000) 1713–1720.
- [107] M.C.D. Mourad, M. Mokhtar, M.G. Tucker, E.R. Barney, R.I. Smith, A.O. Alyoubi, S.N. Basahel, M.S.P. Shaffer, N.T. Skipper, *J. Mater. Chem.* 21 (2011) 15479–15485.
- [108] S. Xu, J.W. Zhao, Q.Q. Yu, X.H. Qiu, K. Sasaki, *ACS Earth Space Chem.* 3 (2019) 2175–2189.
- [109] S. Daniel, P. Alapat, N. Kalarikkal, S. Thomas, *Macromol. Symposia* 398 (2021) 2000277.
- [110] Z. Chang, D.G. Evans, X. Duan, C. Vial, J. Ghanbaja, V. Prevot, M. de Roy, C. Forano, *J. Solid State Chem.* 178 (2005) 2766–2777.
- [111] Y.W. Guo, Z.L. Zhu, Y.L. Qiu, J.F. Zhao, *Chem. Eng. J.* 219 (2013) 69–77.
- [112] S.X. Li, Y.H. Yang, S. Huang, Z.F. He, C.H. Li, D.M. Li, B.H. Ke, C. Lai, Q.Y. Peng, *Appl. Clay Sci.* 188 (2020) 105414.
- [113] K. Warmuz, D. Madej, *Appl. Clay Sci.* 211 (2021) 106196.
- [114] Y. Zhao, Y. Zhao, G.I.N. Waterhouse, L. Zheng, X. Cao, F. Teng, L.Z. Wu, C.H. Tung, D. O'Hare, *T. Zhang, Adv. Mater.* 29 (2017) 1703828.
- [115] S. Iftekhhar, M.E. Kucuk, V. Srivastava, E. Repo, M. Sillanpää, *Chemosphere* 209 (2018) 470–479.
- [116] G. Sheng, Y. Tang, W. Linghu, L. Wang, J. Li, H. Li, X. Wang, Y. Huang, *Appl. Catal. B* 192 (2016) 268–276.
- [117] Y. Wang, Y. Zhang, Z. Liu, C. Xie, S. Feng, D. Liu, M. Shao, S. Wang, *Angew. Chem. Int. Ed.* 56 (2017) 5867–5871.
- [118] H.W.P. Carvalho, S.H. Pulcinella, C.V. Santilli, F. Leroux, F. Meneau, V. Briois, *Chem. Mater.* 25 (2013) 2855–2867.
- [119] S.T. Zhang, Y. Dou, J. Zhou, M. Pu, H. Yan, M. Wei, D.G. Evans, X. Duan, *ChemPhysChem* 17 (2016) 2754–2766.
- [120] Z.P. Xu, G.Q. Lu, *Chem. Mater.* 17 (2005) 1055–1062.
- [121] Z. Gao, K. Sasaki, X. Qiu, *Langmuir* 34 (2018) 5386–5395.
- [122] P. Kowalik, M. Konkol, M. Kondracka, W. Próchniak, R. Bicki, P. Wiercioch, *Appl. Catal. A-General* 464 (2013) 339–347.
- [123] J.J. Bravo-Suárez, E.A. Páez-Mozo, S.T. Oyama, *Quim. Nova* 27 (2004) 601–614.
- [124] R. Allada, A. Navrotsky, H.T. Berbeco, W.H. Casey, *Science* 296 (2002) 721–723.
- [125] J.S. Valente, F. Figueras, M. Gravelle, P. Kumbhar, J. Lopez, J.P. Besse, *J. Catal.* 189 (2000) 370–381.
- [126] S.V. Cherepanova, N.N. Leont'eva, A.B. Arbutov, V.A. Drozdov, O.B. Belskaya, N.V. Antonicheva, *J. Solid State Chem.* 225 (2015) 417–426.
- [127] M.J. Wu, J. Zhang, Y.Q. Peng, J.Z. Zhou, X.X. Ruan, J.Y. Liu, Q. Liu, Y.F. Xi, R. Frost, G.R. Qian, *Microporous Mesoporous Mater.* 242 (2017) 182–189.
- [128] K.K. Rozenberg, Y. Amiel, W.M. Xu, M.P. Pasternak, R. Jeanloz, M. Hanfland, R. D. Taylor, *Phys. Rev. B* 75 (2007) 020102.
- [129] Q.T. Meng, H. Yan, *Mol. Simul.* 43 (2017) 1338–1347.
- [130] Y. Xu, X. Sun, X. Wang, L. He, M.T. Wharmby, X. Hua, Y. Zhao, Y.-F. Song, *Chem. – A Eur. J.* 27 (2021) 13211–13220.
- [131] X. Zhang, J. Shen, Y. Ma, L. Liu, R. Meng, J. Yao, *J. Colloid Interface Sci.* 562 (2020) 578–588.
- [132] A.J. Marchi, C.R. Apesteguía, *Appl. Clay Sci.* 13 (1998) 35–48.
- [133] E. Bazilevskaya, D.D. Archibald, M. Aryanpour, J.D. Kubicki, C.E. Martínez, *Geochim. Cosmochim. Acta* 75 (2011) 4667–4683.
- [134] L. Patrício Cardoso, J.B. Valim, *J. Phys. Chem. Solids* 65 (2004) 481–485.
- [135] S. Miyata, *Clays Clay Miner.* 31 (1983) 305–311.
- [136] X. Qiu, K. Sasaki, S. Xu, J. Zhao, *Langmuir* 35 (2019) 6267–6278.
- [137] L.P. Zhang, X.H. Qiu, J.Y. Chen, *J. Water Process Eng.* 32 (2019) 100987.
- [138] M.P. Bernardo, F.K.V. Moreira, C. Ribeiro, *Appl. Clay Sci.* 137 (2017) 143–150.
- [139] J.J. Bravo-Suárez, E.A. Páez-Mozo, S.T. Oyama, *Quim. Nova* 27 (2004) 574–581.
- [140] L. Xiang, S. Liu, S. Ye, H. Yang, B. Song, F. Qin, M. Shen, C. Tan, G. Zeng, X. Tan, *J. Hazard. Mater.* 420 (2021) 126611.
- [141] M.S. Gasser, H.T. Mohsen, H.F. Aly, *Colloids Surf. A-Physicochem. Eng. Aspects* 331 (2008) 195–201.
- [142] H. He, H. Kang, S. Ma, Y. Bai, X. Yang, *J. Colloid Interface Sci.* 343 (2010) 225–231.
- [143] L. Deng, Z. Shi, X.X. Peng, S.Q. Zhou, *J. Alloy. Compd.* 688 (2016) 101–112.
- [144] T.R. Zhan, Y.M. Zhang, Q. Yang, H.H. Deng, J. Xu, W.G. Hou, *Chem. Eng. J.* 302 (2016) 459–465.
- [145] X. Tong, Z. Yang, P. Xu, Y. Li, X. Niu, *Water Sci. Technol.* 75 (2017) 2194–2203.
- [146] D.S. Tong, M. Liu, L. Li, C.X. Lin, W.H. Yu, Z.P. Xu, C.H. Zhou, *Appl. Clay Sci.* 70 (2012) 1–7.
- [147] M. Suárez-Quezada, G. Romero-Ortiz, V. Suárez, G. Morales-Mendoza, L. Lartundo-Rojas, E. Navarro-Cerón, F. Tzompantzi, S. Robles, R. Gómez, A. Mantilla, *Catal. Today* 271 (2016) 213–219.
- [148] O.D. Pavel, B. Birjega, M. Che, G. Costentin, E. Angelescu, S. Serban, *Catal. Commun.* 9 (2008) 1974–1978.
- [149] J.S. Valente, H. Pfeiffer, E. Lima, J. Prince, J. Flores, *J. Catal.* 279 (2011) 196–204.
- [150] M.G. Álvarez, R.J. Chimentão, N. Barrabés, K. Föttinger, F. Gispert-Guirado, E. Kleymentov, D. Tichit, F. Medina, *Appl. Clay Sci.* 83–84 (2013) 1–11.
- [151] J. Prince, F. Tzompantzi, G. Mendoza-Damian, F. Hernandez-Beltran, J.S. Valente, *Appl. Catal. B-Environ.* 163 (2015) 352–360.

- [152] W.M. Lv, L. Yang, B.B. Fan, Y. Zhao, Y.F. Chen, N.Y. Lu, R.F. Li, *Chem. Eng. J.* 263 (2015) 309–316.
- [153] X. Fang, Y.H. Men, F. Wu, Q.H. Zhao, R. Singh, P. Xiao, T. Du, P.A. Webley, *J. CO₂ Util.* 29 (2019) 57–64.
- [154] E.M. Seftel, M. Puscasu, M. Mertens, P. Cool, G. Carja, *Catal. Today* 252 (2015) 7–13.
- [155] Y.S. Gao, Z. Zhang, J.W. Wu, X.F. Yi, A.M. Zheng, A. Umar, D. O'Hare, Q. Wang, *J. Mater. Chem. A* 1 (2013) 12782–12790.
- [156] W. Li, T.T. Sun, F. Li, *Ind. Eng. Chem. Res.* 53 (2014) 18095–18103.
- [157] X.Y. Zhang, Q.H. Yan, Q. Wang, *Catal. Commun.* 142 (2020) 106037.
- [158] Q.H. Yan, S.N. Chen, C. Zhang, Q. Wang, B. Louis, *Appl. Catal. B-Environ.* 238 (2018) 236–247.
- [159] S. Colonna, M. Bastianini, M. Sisani, A. Fina, *J. Therm. Anal. Calorim.* 133 (2018) 869–879.
- [160] Y.H. Jiang, A.Y. Li, H. Deng, C.H. Ye, Y. Li, *Environ. Sci. Pollut. Res.* 26 (2019) 18343–18353.
- [161] M. Chen, S. Li, L. Li, L. Jiang, Z. Ahmed, Z. Dang, P. Wu, *J. Hazard. Mater.* 401 (2021) 123447.
- [162] L. Hou, X. Li, Q. Yang, F. Chen, S. Wang, Y. Ma, Y. Wu, X. Zhu, X. Huang, D. Wang, *Sci. Total Environ.* 663 (2019) 453–464.
- [163] C. Gong, F. Chen, Q. Yang, K. Luo, F.B. Yao, S.N. Wang, X.L. Wang, J.W. Wu, X.M. Li, D.B. Wang, G.M. Zeng, *Chem. Eng. J.* 321 (2017) 222–232.
- [164] X. Zheng, D. Liu, J. Wen, S. Lv, *Sep. Purif. Technol.* 275 (2021) 117934.